INTRAOPERATIVE QUANTIFICATION OF INTESTINAL MICROCIRCULATION

A modern interpretation of fluorescence angiography

H.G.M. Vaassen

January, 2022

UNIVERSITY OF TWENTE.

INTRAOPERATIVE QUANTIFICATION OF INTESTINAL MICROCIRCULATION

A modern interpretation of fluorescence angiography

MASTER'S THESIS

by

Harry G.M. Vaassen

A thesis submitted in fulfilment of the requirements for the degree of Master of Science in the field of Technical Medicine

January, 2022

Graduation committee

Prof. dr. R.H. Geelkerken

Dr. D.J. Lips

Prof. dr. S. Manohar

B. Wermelink, MSc.

Drs. P.A. van Katwijk

J.K. van Zandwijk, MSc.

Cover artwork: E.M. Heijmans

Abstract

Background – Intraoperative assessment of local intestinal perfusion is critical for evaluating bowel vitality and preventing anastomotic complications. In current practice, surgeons employ subjective and inaccurate methods, relying on clinical signs. Fluorescence angiography (FA) allows immediate tracing of blood flow, but the subjective interpretation of images has been inadequate in reducing perfusion related complications. The work in this thesis is dedicated to developing an FA-based technique that enables reliable quantification of intestinal perfusion levels and aids surgeons with intraoperative decision-making.

Methods – Algorithms were designed to quantify the inflow of contrast agent indocyanine green in tissue, and accompanying software was developed to perform this intraoperatively. The behaviour and comparability of two near-infrared (NIR) acquisition systems were investigated in-vitro. A clinical pilot study was initiated to evaluate the (potential) clinical value of two quantified FA parameters. In order to provide a healthy reference frame, FA data was obtained in 32 patients without bowel perfusion impairment. Measurements were subsequently performed in nine patients with a diagnosed form of impaired bowel perfusion. Seven of these patients underwent revascularization, after which FA was performed once more.

Results and Discussion – In-vitro experiments revealed unpredictable behaviour in one of the NIR acquisition systems. However, inflow-based FA quantification in a dynamic perfusion phantom was reasonably comparable. Algorithm validation using more sophisticated phantoms and the use of unprocessed NIR signals are advised before threshold values for clinical decision-making are pursued.

In the clinical pilot study, median values of inflow parameters differed significantly from those of the healthy group ($P < 0.01$). Moreover, six of the seven patients who underwent revascularization showed a clear recovery of the parameters into the healthy range after intervention. Using our developed technique, bowel perfusion impairment that was not observed on clinical inspection could be detected. These findings illustrate a great potential value. Further studies should define threshold values for various perfusion requirements.

Contents

List of Abbreviations

AF	Atrial fibrilation
AL	Anastomotic leakage
AMI	Acute mesenteric ischemia
AoCMI	Acute-on-chronic mesenteric ischemia
ASA	American Society of Anesthesiologists
BMI	Body Mass Index
CA	Celiac artery
CCD	Charge-coupled device
CHA	Common hepatic artery
CI	Confidence interval
CIA	Common iliac artery
CMI	Chronic mesenteric ischemia
CMOS	Complementary metal oxide semiconductor
CT	Computed tomography
CVA	Cerebro-vascular accident
DM2	Type 2 Diabetes Mellitus
DUS	Doppler ultrasonography
DVT	Deep vein thrombosis
EIA	External iliac artery
FA	Fluorescence angiography
FIR	Finite impulse response
FLIGHT	FLuorescence Imaging for Gastrointestinal Hemodynamics Trial
HL	Hyperlipidaemia
HT	Hypertension
GI	Gastrointestinal
ICC	Intraclass correlation
ICG	Indocyanine green
IQR	Interquartile range
IMA	Inferior mesenteric artery
IMV	Inferior mesenteric vein
LDF	Laser doppler flowmetry
MST	Medisch Spectrum Twente
NIR	Near-infrared
NPS	Normalized peak slope
PAD	Peripheral artery disease
PPG	Photopletysmography
PS	Peak slope
RGB	Red-green-blue colourcoding
ROI	Region of interest
SBS	Small bowel strangulation
SD	Standard deviation
SMA	Superior mesenteric artery
SMV	Superior mesenteric vein
TTP	Time to peak

1 General introduction

In a wide field of surgical disciplines, knowledge of organ perfusion is critical. Gastro-intestinal surgery is no exception, since compromised bowel perfusion can result in one of the most dreaded postoperative complications: leakage of an anastomosis. With incidences reported between 3 and 22% depending on the procedure, many patients suffer the consequences that include re-intervention, extended hospital stay and even death. Moreover, perfusion impairment of the bowel can reach the extent that tissue becomes necrotic. Resection of the affected segment might be necessary in these cases, but this critical decision is made based solely on surgical experience. In any event, surgeons are guided by clinical signs without objective knowledge on the perfusion status.

Throughout history, the increasing use of objective and quantifiable data has transformed clinical medicine from a conjectural art into a scientific discipline, embodied by the term *'evidence-based medicine'*. Bearing this in mind, the currently employed indicators for intestinal perfusion, such as tissue colour and pulsations, seem obsolete and are due for a modernization.

Initially developed as a photographic dye during the Second World War, indocyanine green (ICG) has been adapted by the medical community due to its fluorescent properties for decades. ICG can be injected intravenously and act as a tracer of blood flow, facilitating a technique dubbed as fluorescence angiography (FA). Modern equipment and technological advances have made FA a widely available and straightforward technique to evaluate local perfusion dynamics. Nonetheless, intraoperative perfusion assessment by means of FA has, as of yet, not experienced its expected clinical breakthrough. In its current form, FA is merely a technologically advanced addition to the surgeon's qualitative toolbox, leaving plenty of room for subjective interpretation. Besides, measurement circumstances can make FA images deceiving for the inexperienced user.

Having said that, FA can provide insights in local blood flow that cannot be acquired with the naked eye. It has therefore, when proper quantification is achieved, the potential to be a powerful instrument in the pursuit of decreasing perfusion-related complications.

1.1 Aim and outline

The work presented in this thesis was dedicated to creating a peroperative tool for quantification of intestinal perfusion by means of FA. Ultimately, the aim was to obtain a method that can be implemented in the operating theatre and is ready for validation in clinical trials. Chapter 2 outlines the clinical and technical background regarding intestinal perfusion and FA. Technical specifics with respect to analysis strategies and software development are addressed in Chapter 3. In Chapter 4, an in vitro study involving a dynamic perfusion phantom is portrayed. Chapter 5 presents a peer-reviewed publication that describes the first efforts of automated FA quantification in our group. Chapter 6 contains a submitted manuscript that presents a state-of-art method for on-site FA analysis and explores the clinical potential by means of a pilot study. In Chapter 7, an overall summary of findings is provided along with a general discussion and section on future perspectives.

2 Background

The following paragraphs provide a background on the anatomy and pathology of intestinal circulation, and illustrate why surgeons are in need of new methods to assess it intraoperatively.

2.1 Anatomy

2.1.1 Small intestine[1]

The small intestine, part of the alimentary or digestive system, is a tubular structure and consists of three parts. The duodenum extends from the pylorus of the stomach and has a length of approximately 25 cm. Based on its orientation, it is divided into four sections: a superior, descending, inferior and ascending part. The descending part of duodenum is home to the major duodenal papilla, where the pancreatic and biliary system are drained. The transition into the jejunum, the duodenojejunal flexure, is suspended to the diaphragm by Treitz's ligament. With exception from the first few centimetres, the duodenum lies retroperitoneal. The intraperitoneal jejunum and ileum form the largest part of the small intestine, with a combined length of approximately 3-5 metres. Most of the absorption of nutrients and minerals is carried out in these structures. There is no clear transition point of jejunum into ileum, but they have distinctive attributes, with the jejunum presenting a thicker wall, larger arterial arcades and longer vasa recta. The ileum, and thereby the whole small intestine, ends in the cecum of the large intestine.

The wall of the small intestine is constructed of several layers (see Fig. 1.1):

1. Visceral peritoneum or serosa.
2. Subserosa
3. Muscularis externa, consisting of a longitudinal and circular layer of muscle fibres, with the myenteric (Auerbach's) plexus in between. The nerves and muscle fibres in this layer orchestrate bowel motility.
4. Submucosa with submucosal (Meissner's) plexus, which innervates the lamina muscularis mucosae and the mucosa.
5. Muscularis mucosae, containing a longitudinal and circular layer of muscle fibres. This layer has great influence on the absorptive and secretory functions of the epithelium.[2]
6. Mucosa, consisting of lamina propria and epithelium.

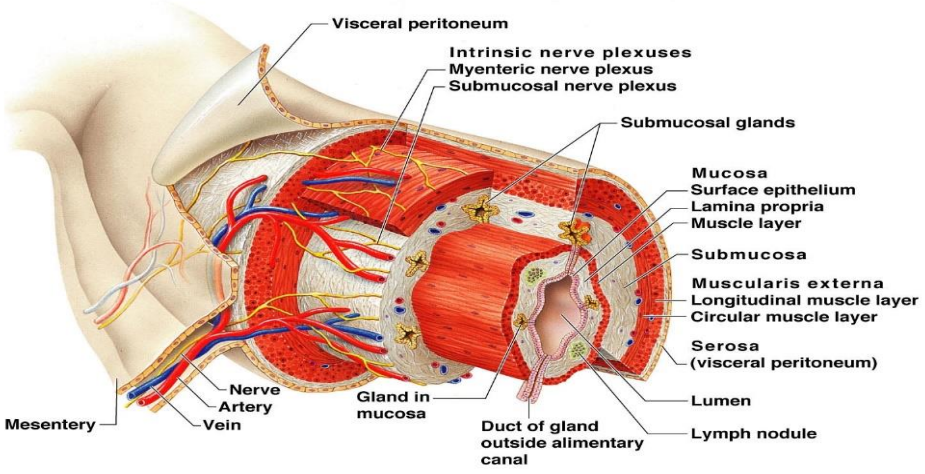

Figure 2.1. *Layers of the small intestine (by courtesy of Pearson Education, Inc. 2009)*

2.1.2 Large intestine[1]

The large intestine consists of the cecum with the appendix, the four parts of the colon and the rectum with anal canal. It is distinguishable from the small intestine, mainly due to the thickened bands of external longitudinal muscle fibres (teniae coli) and the sacculations (haustra) caused by the teniae coli. The ileum enters the first part of the large intestine in the ileocecal junction, which contains the ileocecal valve. The colon continues directly from the cecum in the right lower quadrant. Its first part, the ascending colon, passes along the right side of the abdomen towards the liver. Just below the liver, it turns left to join the transverse colon via the hepatic flexure. The transverse colon crosses the upper part of the abdomen from right to left before it turns inferiorly into the descending colon via the splenic flexure. The final part of the colon, the sigmoid, originates from the descending colon in the left lower quadrant and connects to the rectum. It is characterized by its S-shape. The rectum and anal canal form the terminal part of the large intestine.

2.2 Abdominal vascularization

2.2.1 Arterial supply

Most structures in the abdomen are provided with oxygenated blood by three main branches of the abdominal aorta. The most superior of these branches is the celiac trunk, which branches into the left gastric, common hepatic and splenic arteries. The first two parts of the duodenum are supplied by the gastroduodenal artery, a branch from the common hepatic artery, and one of its branches, the superior pancreaticoduodenal artery. A branch from the superior mesenteric artery (SMA), the inferior pancreaticoduodenal artery, supplies the inferior and ascending part of the duodenum. This construction provides a connection between celiac and SMA blood supply, allowing collateral circulation when necessary.

The jejunum and ileum are supplied of blood by 15-18 branches of the SMA. These arteries connect with each other to form arterial arcades, from which the vasa recta extend towards the intestine. The terminal part of the ileum and the cecum receive blood from the SMA through the ileocolic artery. The left colic and middle colic artery, supplying the ascending and transverse colon respectively, are branches from the SMA as well. Another branch from the abdominal aorta,

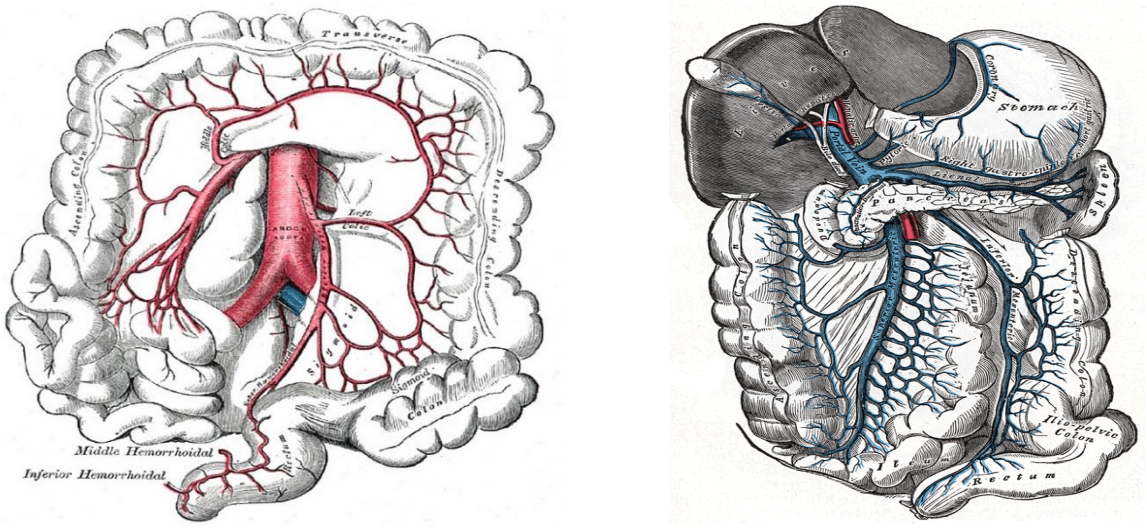

Figure 2.2. ***Left*** *Superior and inferior mesenteric artery originating from the abdominal aorta and branching out to supply the colon. Duodenal and jejunal branches are not illustrated.* ***Right*** *Drainage of the gastrointestinal tract through the superior and inferior mesenteric vein into the splenic vein and portal system.*

the inferior mesenteric artery (IMA), supplies the remaining distal part of the gastrointestinal tract up to and including the proximal part of the rectum. The descending and sigmoid colon are supplied by the left colic and sigmoid arteries, branches of the IMA. In most cases, the colic arteries anastomose with each other proximal to the colon, forming an arcade (marginal artery of Drummond). Near the splenic flexure, where the colonic blood supply transitions from SMA origin into IMA origin, this arcade offers important collateral blood flow between SMA and IMA. The arc of Riolan (mesenteric meandering artery) is a similar collateral arcade between SMA and IMA, found more central in the mesentery.[3]

2.2.2 Venous drainage

Similar to arterial supply, venous drainage of the small and large intestine (with exception from the proximal duodenum) happens through a superior and inferior mesenteric vein (SMV, IMV). The transition between the two is around the splenic flexure as well. The IMV drains into the splenic vein, which also receives inflow from short gastric, left gastroepiploic and pancreatic veins. The SMV joins the splenic vein to transport blood to the liver through the portal vein.

2.3 Mesenteric ischemia

2.3.1 Cause

Mesenteric circulation can be distorted by several causes. Of these, arterial obstruction is the most common. Acute mesenteric ischemia (AMI) is associated with embolic occlusion in 40-50% of cases and with thrombotic occlusion of a stenotic mesenteric vessel in 20-35% of cases. Chronic mesenteric ischemia (CMI) is in 90% of cases the result of progressive atherosclerotic disease.[4] Mesenteric venous thrombosis is responsible for 5-15% of mesenteric ischemia cases. It has a wide variety of causes, but in most instances it seems to be a combination of hypercoagulable state and some sort of event, such as infection or surgery. The IMV is rarely involved in mesenteric venous thrombosis. An increasing number of patients are identified through unrelated imaging diagnostics to have venous thrombosis.[5] In 5-15% of mesenteric ischemia diagnoses, occlusion is not the underlying pathology (nonocclusive mesenteric ischemia). These cases are generally associated with low-flow states due to for instance cardiac insufficiency or hypovolemia.

The most common presentation of gastrointestinal hypoperfusion is ischemic colitis. In 80-85% of ischemic colitis patients, the condition is non-gangrenous and clinical consequences are relatively mild. However, the remainder of patients can experience very serious complications, such as severe abdominal pain, peritonitis and ileus, and are subjected to extremely high mortality rates (up to 75%).[6]

2.3.2 Symptoms and diagnosis

CMI patients commonly present with postprandial abdominal pain with, as a result, food aversion and consequential weight loss. In case of AMI, patients generally suffer from severe abdominal pain, vomiting and (bloody) diarrhoea. Although (CT) angiography has great sensitivity in detecting mesenteric vessel stenoses and occlusions, diagnosis of CMI and AMI is not straightforward. Many of the accompanying symptoms are not specific for mesenteric ischemia, and mesenteric vessel stenoses are observed on CT in the general population at a rate of 18%. For this reason, clinicians often rely on an invasive function test to confirm CMI. Often, AMI is not recognized on first presentation. Since the first hours after onset of symptoms are critical, this underdiagnosis contributes to the extremely high mortality rates of AMI (50-69%). [7]

2.3.3 Treatment

In some cases of mesenteric ischemia, intervention is not required. Conservative treatment is mainly focussed on suppressing the progression of atherosclerosis and minimizing mesenteric oxygen demand. Nevertheless, revascularization is indicated in most cases of chronic and acute mesenteric ischemia. Blood supply can be improved by means of endovascular approaches (angioplasty and/or stent placement), open surgical repairs (endarterectomy or bypass) and hybrid techniques (retrograde open mesenteric stenting).[8,9]

In the event of AMI or acute-on-chronic mesenteric ischemia, bowel is at risk. The main goal of treatment is intestinal salvage. According to the guidelines, blood flow should be restored at first. Signs of peritonitis demand laparotomy, where bowel vitality can be assessed and gangrenous segments resected.[10] The extent of the resection is a crucial but complicated concern. Necrotic bowel should clearly be resected, but reversibility of ischemia is, even in experienced hands, hard to judge in remaining segments without insights on local perfusion status. Moreover, bowel resection comes at a price for the patient. The surgeon may be hesitant to resect additional bowel without a clear diagnosis of ischemia in order to avoid short bowel syndrome and the complications that go along with it, including intestinal failure and the need for lifelong parental nutrition. However, the fatal consequences of leaving inviable bowel, including peritonitis and sepsis, motivate surgeons to be liberal with resections. Partly due to this fact, 30% of patients undergoing ischemic bowel resection develop short bowel syndrome.[11]

2.4 Gastrointestinal surgery

Vascular surgeons are not alone in their desire to gain knowledge on intestinal perfusion levels during procedures. Many gastrointestinal (GI) interventions entail the construction of anastomoses to ensure continuity of the GI tract. Here, one of the most feared postoperative complications is anastomotic leakage (AL). In spite of great advancements in surgical technique, AL rates are still reported between 3 and 19% in colorectal surgery.[12,13] In upper GI surgery, AL rates are reported up to 22%. The consequences of AL can be catastrophic and include extended hospital stay, re-intervention and peritonitis, while mortality rates have been reported up to 16%.[14] Several factors, such as anastomotic tension and nutrition level, influence gastrointestinal healing, but local perfusion is widely regarded as most important.[15] Better insights on local perfusion dynamics should therefore decrease the considerable incidence rates of AL in GI surgery.

GI-surgeons might also be presented with compromised bowel segments at risk for necrosis. Examples are small bowel strangulation due to adhesions and incarcerated herniations. Often, the extent of the affected segment is less than that in case of advanced AMI, so there is less risk of short bowel syndrome. Bowel resection remains, nevertheless, an invasive intervention associated with increased morbidity, so it should be avoided whenever possible. Again, knowledge on perfusion and reversibility of ischemia could improve intraoperative decisions significantly.

2.5 Peroperative assessment of bowel perfusion

2.5.1 Clinical observation

Proper evaluation of intestinal blood supply is imperative during abdominal surgery. In general, surgeons are trained to observe clinical signs, such as serosal colour, marginal artery pulsations and peristalsis. This approach introduces subjectivity and relies on surgical experience. Besides, the mentioned signs can be deceptive. For example, early arterial insufficiency may go completely unnoticed, while viable bowel that is burdened by minor venous congestion might show evident dark discoloration.[16] Systemic hypotension or spasms could falsely suggest impaired mesenteric circulation, due to a lack of palpable pulsations in the mesentery, and grossly ischemic bowel might even display peristalsis. [17,18] In case of laparoscopic surgery, resources are further limited to visual inspection only. This is the main reason why a minimally invasive approach is generally not recommended in the treatment of small bowel strangulations.[19]

2.5.2 Technological aids

Various technologies have been investigated to aid in peroperative assessment of bowel vitality and perfusion. Early adapted techniques include photoplethysmography (PPG), doppler ultrasonography (DUS) and laser doppler flowmetry (LDF). PPG, or pulse oximetry, measures oxygen saturation in tissue based on absorbance of light. Although a clear relation between oxygenation values and intestinal viability has been demonstrated in animal models, literature has remained conflicted on intraoperative applicability and efficacy. The limited penetration depth makes it, for instance, only able to detect transmural ischemia, while early mucosal necrosis would remain undetected. Moreover, additional studies have reported high rates of false-negative and false-positive results.[20,21]

DUS and LDF aim to detect the movement of erythrocytes by measuring a frequency change when sound or light is reflected by them. Especially DUS has found its way into vascular surgery, due to low costs and its non-invasive nature. It is, however, more suitable for the assessment of macrovasculature than for microcirculatory perfusion. Moreover, the highly variable measurements have made quantitative analysis unfeasible. LDF has more quantitative potential, and its use led to less perioperative complications in patients with AMI compared with clinical judgement alone in previous studies. Nonetheless, LDF has failed to reach introduction in the surgical workflow due to poor integrability as a result of motion artefacts and time-consuming measurements. Similar problems have withheld another optical technique, laser speckle contrast imaging, from implementation in gastrointestinal surgery.[17,21]

2.6 Clinical need

All things considered, there is a clear need for a new method that facilitates *reliable* and *objective* peroperative assessment of intestinal perfusion. In recent years, research in intestinal perfusion assessment has been shifting towards the use of intravenously admitted fluorescent dyes. The following paragraphs provide a technical background regarding fluorescence imaging, specifically angiography, and an overview of the current state-of-art.

2.7 Fluorescence imaging

2.7.1 Physical principle

Fluorescence is a type of photoluminescence that involves light emitted by an atom or molecule after the absorption of electromagnetic energy. The absorbed light promotes an electronic transition between the ground state and a certain excited state. Relaxation back to the ground state can happen through several mechanisms, illustrated by the Jablonski diagram in Figure 2.3. One way of relaxation is trough the emittance of a photon (radiative transition), which is called fluorescence in case of direct transition without change in spin state. This usually happens after some of the energy is lost trough internal conversion into heat. Due to this loss, the emitted fluorescence photon has a lower energy, and thus a longer wavelength, than the one that induced initial excitation (redshift). Direct relaxation happens within a very short time after excitation, meaning that fluorescence stops almost instantly after removal of the excitation source. If electrons undergo intersystem crossing, meaning they transition between spin multiplicity states, their decay back to the ground state occurs much slower. A radiative transition during this decay can therefore happen much longer after initial excitation, creating a phenomenon called phosphorescence.

2.7.2 Indocyanine green

Since its introduction, contrast agent indocyanine green (ICG) has been widely used in biomedical fields. ICG is an attractive agent, due to its low toxicity and extravasation-preventing lipophilic qualities. In addition, the excitation and emission spectra are subjected to a relatively high transparency in biological tissue.[22,23] Solved in blood, maximum absorption happens at approximately 800 nm and the peak of the emission spectrum lies at approximately 830-840 nm. Both of these wavelengths are categorized as near-infrared (NIR). In most appliances, excitation is performed using wavelengths around 780 nm, so fluorescent light can be distinguished from the scattered excitation beam more easily. The imaging technique is illustrated in Figure 2.4. ICG can be detected at a maximum depth between 1 and 2 cm, depending on the tissue. After injection in the bloodstream, ICG is quickly metabolized by the liver and excreted through the biliary system. ICG has a wide field of applications, including ophthalmology, liver function tests and image-guided oncologic surgery.

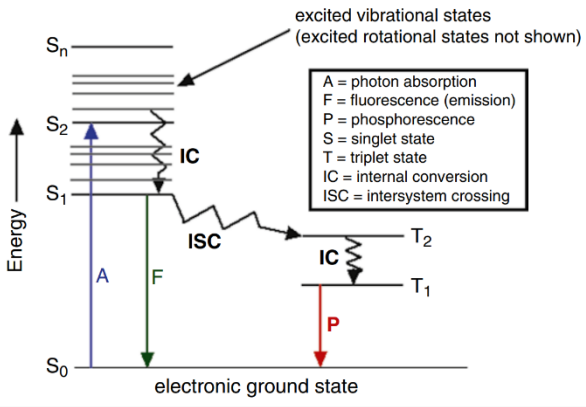

Figure 2.3. *Jablonski diagram, representing the various pathways of relaxation after excitation due to photon absorption.*

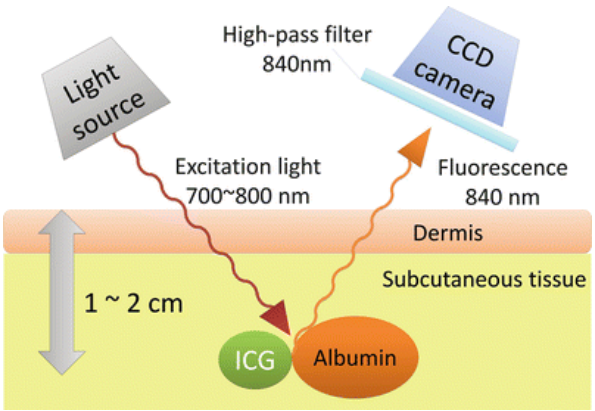

Figure 2.4. *Near-infrared excitation and detection of ICG in tissue.*

2.7.3 Dynamic imaging

If ICG is injected intravenously as a bolus, it travels through the entire circulatory system before a first passage through the liver. It can therefore be used as a tracer of blood flow, enabling assessment of local tissue perfusion. This method is known as fluorescence angiography (FA).

FA has found its way into gastrointestinal surgery, and its role in peroperative decision-making has already been demonstrated.[24–27] In 2015, FA was performed on 139 colorectal surgery patients in the PILLAR II trial. FA initiated relocation of the initially planned transection line in 8% of patients.[27] In a later stage, Kawada et al. presented a change in surgical plans after FA in 26.5% of colorectal surgery patients.[24] In both studies, the reported rate of AL (1.4% and 4.5% respectively) was lower than those found in literature, indicating that the use of FA might have a decreasing effect on AL risks. Moreover, the superiority of FA over judgement on clinical signs alone in the detection of perfusion impairment has been shown in animal models.[28,29]

Nevertheless, randomized control trials are in disagreement on the capability of FA in preventing anastomotic leakage. Alekseev et al. found significant reduction in colorectal AL after FA ($P = 0.04$), but research by De Nardi et al. did not provide such an association.[26,30] Similar to assessment based on clinical signs, FA image interpretation involves great subjectivity. Moreover, in addition to local perfusion levels, the acquired data depends on many factors like light-source distance, ICG dosing, angulation etc. This makes the interpretation deceptive, especially for inexperienced users.[31,32] Several reviews have therefore stated that the current qualitative interpretation of FA data is not adequate, and that there is a need for objective quantified FA.[33–35]

2.7.4 Quantified FA

Quantitative FA parameters obviate the subjectivity and lack of repeatability that is involved with qualitative interpretation. They are extracted from an 'intensity-time curve', created by measuring the pixel intensity in a specific region of interest during the FA recording (see Fig. 2.5). The parameters calculated from this signal can be divided into two categories. Intensity-based parameters provide a measure on the amount of ICG present in the tissue, since a greater quantity of ICG results in more photons. An example is the maximal intensity F_{max}. Similar to qualitative interpretation, FA intensity values are subject to measurement circumstances. Factors like light-source to camera distance, ICG dosing, camera direction and reflections all influence the result, and it is unfeasible to exactly correct for or control these elements in an operative setting. This

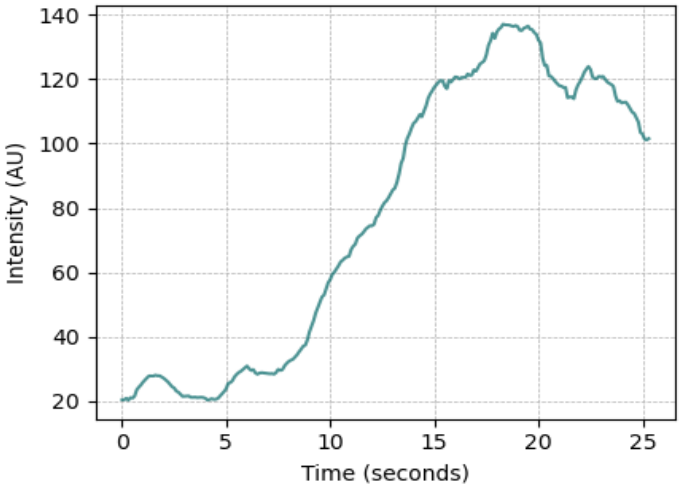

Figure 2.5. *Typical FA intensity-time curve in small bowel*

Table 2.1. Quantified FA parameters for the detection of AL in studies by Son et al. and Wada et al.

Authors	AL	F_{max} (AU)	T_{max} (AU)	$T_{1/2}$ (s)	$Slope$ $(^{AU}/_{s})$
Son et al.[38]	(-) $(n = 80)$	58.0 ± 3.4	30.3 ± 2.3	11.7 ± 0.8	2.5 ± 0.2
	(+) $(n = 6)$	34.9 ± 7.4	64.0 ± 11.7	40.4 ± 7.8	0.7 ± 0.2
	P-value	0.820	<0.001	<0.001	<0.001
Wada et al.[37]	(-) $(n = 107)$	91.4 ± 31.9	32.8 ± 15.9	12.5 ± 7.6	3.6 ± 0.2
	(+) $(n = 5)$	38.1 ± 11.5	52.1 ± 28.5	26.1 ± 18.9	1.0 ± 0.7

makes the interpretation of measurements complicated and unreliable, and advocates the use of time-based (or inflow) parameters for the quantification of FA. Examples of these parameters are $T_{1/2}$ (time to reach 50% of maximal intensity) and slope (gradient of the intensity increase, which is also intensity-based but can be normalized). Inflow-based parameters are considerably less dependent on measurement circumstances.

For the identification of impaired perfusion based on quantified FA, parameters should be comparable between patients, rendering inflow-based quantification the superior approach. In an ex vivo animal model, Nerup et al. showed a strong correlation between the maximal slope of the intensity time signal and regional blood flow ($r = 0.97, P < 0.001$). Neutron-activated microspheres were used as the golden standard in this model.[36] Likewise, the ability of FA to detect boundaries between ischemic and vascular zones was shown in a pig model by Diana et al.[28] A few in vivo studies have illustrated the potential value of quantified FA as well. Studies by Son et al. and Wada et al. investigated the predictive value of several parameters with respect to anastomotic leakage after colorectal resections.[37,38] Their reported values are presented in Table 2.1. One of the most noticeable findings in this table is the great variation in maximal intensity between the two studies. Again, the lack of reproducibility of intensity-based parameters is illustrated. $T_{1/2}$ emerged as the best predictor of anastomotic leakage in these studies, with reported sensitivities of 80% and 100% and specificities of 74% and 84%. However, the number of AL cases was relatively low in both studies. A larger number of patients with impaired perfusion need to be included in analysis, in order to obtain reliable information on the parameters. Moreover, the greater standard deviations in the study by Wada et al. suggest a difference in data interpretation methods between the studies.

2.7.5 Technical challenge

From a theoretical point of view, inflow-based parameters provide more consistent and comparable measurements than the often reported intensity-based parameters. This is supported by research in animal models and by small retrospective in vivo studies.[28,37–39] However, these parameters are less straightforward to determine, and often require off-line manual analysis. Moreover, ambiguities exist on the exact definition of several points of interest, such as the start- and endpoint of the intensity increase.[40,41] Current methods of quantification are inadequate and require enhancement to be applicable in an intraoperative setting.

2.8 Objectives

The main objective that will be pursued in this thesis is the transformation of FA into a reliable and objective peroperative tool for intraoperative quantification of intestinal perfusion. For this purpose, the following issues will be addressed:

- Automatic and reliable extraction of inflow-based parameters from FA data.
- Integration of quantified FA in the operative workflow.
- Evaluation of the clinical accuracy and potential regarding impaired intestinal perfusion.

References

1. Moore KL, Dalley AF, Agur AMR. Clinically Oriented Anatomy, 8e. 2018.
2. Uchida K, Kamikawa Y. Muscularis mucosae - The forgotten sibling. Vol. 43, Journal of Smooth Muscle Research. J Smooth Muscle Res; 2007. p. 157–77.
3. Walker TG. Mesenteric vasculature and collateral pathways. Semin Intervent Radiol. 2009 Sep;26(3):167–74.
4. Clair DG, Beach JM. Mesenteric Ischemia. Campion EW, editor. N Engl J Med. 2016 Mar 10;374(10):959–68.
5. Kumar S, Sarr MG, Kamath PS. Mesenteric Venous Thrombosis. N Engl J Med. 2001 Dec 6;345(23):1683–8.
6. Nikolic AL, Keck JO. Ischaemic colitis: uncertainty in diagnosis, pathophysiology and management. ANZ J Surg. 2018;88(4):278–83.
7. Tilsed JVT, Casamassima A, Kurihara H, Mariani D, Martinez I, Pereira J, et al. ESTES guidelines: acute mesenteric ischaemia. Vol. 42, European Journal of Trauma and Emergency Surgery. 2016. p. 253–70.
8. Hohenwalter EJ. Chronic mesenteric ischemia: Diagnosis and treatment. Semin Intervent Radiol. 2009;26(4):345–51.
9. Blauw JTM, Meerwaldt R, Brusse-Keizer M, Kolkman JJ, Gerrits D, Geelkerken RH. Retrograde open mesenteric stenting for acute mesenteric ischemia. J Vasc Surg. 2014;60(3):726–34.
10. Björck M, Koelemay M, Acosta S, Bastos Goncalves F, Kölbel T, Kolkman JJ, et al. Editor's Choice e Management of the Diseases of Mesenteric Arteries and Veins Clinical Practice Guidelines of the European Society of Vascular Surgery (ESVS). 2017;
11. Karampinis I, Keese M, Jakob J, Stasiunaitis V, Gerken A, Attenberger U, et al. Indocyanine Green Tissue Angiography Can Reduce Extended Bowel Resections in Acute Mesenteric Ischemia. J Gastrointest Surg. 2018 Dec 1;22(12):2117–24.
12. Platell C, Barwood N, Dorfmann G, Makin G. The incidence of anastomotic leaks in patients undergoing colorectal surgery. Color Dis. 2007;9(1):71–9.
13. Kingham TP, Pachter HL. Colonic Anastomotic Leak: Risk Factors, Diagnosis, and Treatment. J Am Coll Surg. 2009;208(2):269–78.
14. Li YW, Lian P, Huang B, Zheng HT, Wang MH, Gu WL, et al. Very Early Colorectal Anastomotic Leakage within 5 Post-operative Days: A More Severe Subtype Needs Relaparatomy. Sci Rep. 2017;7(November 2016):1–7.
15. Thompson SK, Chang EY, Jobe BA. Clinical review: Healing in gastrointestinal anastomoses, part I. Vol. 26, Microsurgery. 2006. p. 131–6.
16. Geelkerken RH, Cannegieter SC, Bouter H, van Bockel JH. Acute splanchnic venous thrombosis: surgical and medical treatment with special emphasis on new aspects of coagulation disorders. Eur J Vasc Endovasc Surg. 1997;13(2):227–32.
17. Urbanavičius L. How to assess intestinal viability during surgery: A review of techniques. World J Gastrointest Surg. 2011;3(5):59.
18. La Hei ER, Shun A. Intra-operative pulse oximetry can help determine intestinal viability. Pediatr Surg Int. 2001;17(2–3):120–1.
19. Guerra F, Coletta D, Greco PA, Eugeni E, Patriti A. The use of indocyanine green fluorescence to define bowel microcirculation during laparoscopic surgery for acute small bowel obstruction. Color Dis. 2021;23(8):2189–94.
20. Dyess DL, Bruner BW, Donnell CA, Ferrara JJ, Powell RW. Intraoperative evaluation of intestinal ischemia: A comparison of methods. South Med J. 1991;84(8):966–9.

21. Bryski MG, Frenzel Sulyok LG, Kaplan L, Singhal S, Keating JJ. Techniques for intraoperative evaluation of bowel viability in mesenteric ischemia: A review. Am J Surg. 2020;220(2):309–15.

22. Yuan B, Chen N, Zhu Q. Emission and absorption properties of indocyanine green in Intralipid solution. J Biomed Opt. 2004;9(3):497.

23. van den Biesen PR, Jongsma FH, Tangelder GJ, Slaaf DW. Yield of fluorescence from indocyanine green in plasma and flowing blood. Ann Biomed Eng. 1995;23(4):475–81.

24. Kawada K, Hasegawa S, Wada T, Takahashi R, Hisamori S, Hida K, et al. Evaluation of intestinal perfusion by ICG fluorescence imaging in laparoscopic colorectal surgery with DST anastomosis. Surg Endosc. 2017;31(3):1061–9.

25. Su H, Wu H, Bao M, Luo S, Wang X, Zhao C, et al. Indocyanine green fluorescence imaging to assess bowel perfusion during totally laparoscopic surgery for colon cancer. BMC Surg. 2020;20(1):1–7.

26. De Nardi P, Elmore U, Maggi G, Maggiore R, Boni L, Cassinotti E, et al. Intraoperative angiography with indocyanine green to assess anastomosis perfusion in patients undergoing laparoscopic colorectal resection: results of a multicenter randomized controlled trial. Surg Endosc. 2020;34(1):53–60.

27. Jafari MD, Wexner SD, Martz JE, McLemore EC, Margolin DA, Sherwinter DA, et al. Perfusion assessment in laparoscopic left-sided/anterior resection (PILLAR II): A multi-institutional study. J Am Coll Surg. 2015;220(1):82-92.e1.

28. Diana M, Noll E, Diemunsch P, Dallemagne B, Benahmed MA, Agnus V, et al. Enhanced-reality video fluorescence: A real-time assessment of intestinal viability. Ann Surg. 2014;259(4):700–7.

29. Matsui A, Winer JH, Laurence RG, Frangioni J V. Predicting the survival of experimental ischaemic small bowel using intraoperative near-infrared fluorescence angiography. Br J Surg. 2011;98(12):1725–34.

30. Alekseev M, Rybakov E, Shelygin Y, Chernyshov S, Zarodnyuk I. A study investigating the perfusion of colorectal anastomoses using fluorescence angiography: results of the FLAG randomized trial. Color Dis. 2020;22(9):1147–53.

31. Hardy NP, Dalli J, Khan MF, Andrejevic P, Neary PM, Cahill RA. Inter-user variation in the interpretation of near infrared perfusion imaging using indocyanine green in colorectal surgery. Surg Endosc. 2021;

32. Dalli J, Hardy N, Mac Aonghusa PG, Epperlein JP, Cantillon Murphy P, Cahill RA. Challenges in the interpretation of colorectal indocyanine green fluorescence angiography – A video vignette. Vol. 23, Colorectal Disease. 2021. p. 1289–90.

33. Degett TH, Andersen HS, Gögenur I. Indocyanine green fluorescence angiography for intraoperative assessment of gastrointestinal anastomotic perfusion: a systematic review of clinical trials. Langenbeck's Arch Surg. 2016;401(6):767–75.

34. Jansen-Winkeln B, Germann I, Köhler H, Mehdorn M, Maktabi M, Sucher R, et al. Comparison of hyperspectral imaging and fluorescence angiography for the determination of the transection margin in colorectal resections—a comparative study. Int J Colorectal Dis. 2021 Feb 1;36(2):283–91.

35. Slooter MD, Eshuis WJ, Cuesta MA, Gisbertz SS, van Berge Henegouwen MI. Fluorescent imaging using indocyanine green during esophagectomy to prevent surgical morbidity: A systematic review and meta-analysis. J Thorac Dis. 2019;11(1):S755–65.

36. Nerup N, Andersen HS, Ambrus R, Strandby RB, Svendsen MBS, Madsen MH, et al. Quantification of fluorescence angiography in a porcine model. Langenbeck's Arch Surg. 2017;402(4):655–62.

37. Wada T, Kawada K, Takahashi R, Yoshitomi M, Hida K, Hasegawa S, et al. ICG fluorescence imaging for quantitative evaluation of colonic perfusion in laparoscopic colorectal surgery. Surg Endosc. 2017;31(10):4184–93.

38. Son GM, Kwon MS, Kim Y, Kim J, Kim SH, Lee JW. Quantitative analysis of colon perfusion pattern using indocyanine green (ICG) angiography in laparoscopic colorectal surgery. Surg Endosc. 2019;33(5):1640–9.

39. Nerup N, Svendsen MBS, Svendsen LB, Achiam MP. Feasibility and usability of real-time intraoperative quantitative fluorescent-guided perfusion assessment during resection of gastroesophageal junction cancer. Langenbeck's Arch Surg. 2020;405(2):215–22.

40. Meijer RPJ, van Manen L, Hartgrink HH, Burggraaf J, Gioux S, Vahrmeijer AL, et al. Quantitative dynamic near-infrared fluorescence imaging using indocyanine green for analysis of bowel perfusion after mesenteric resection. J Biomed Opt. 2021;26(06):1–8.

41. Lütken CD, Achiam MP, Svendsen MB, Boni L, Nerup N. Optimizing quantitative fluorescence angiography for visceral perfusion assessment. Surg Endosc. 2020;34(12):5223–33.

3 Methods of analysis

3.1 Intensity signal

In MST, two NIR imaging systems are available for FA: the Firefly module of the DaVinci X robotic surgery system (Intuitive Surgical, Sunnyvale, CA, USA) and the monochromatic NIR module of the Storz laparoscopy system (Karl Storz, GmbH and Co., KG, Tüttlingen, Germany). Quantification of FA data is based on intensity-time curves. Since neither of the available systems provides radiometric data, intensity values need to be extracted from the RGB video output (live frames or MP4 recording). Based on the way fluorescent signals are displayed on these systems, intensity values are extracted in different ways. The intensity value I is determined by the green channel in case of the DaVinci system:

$$I = G \tag{3.1}$$

For the Storz system, the luminance value Y is calculated according to:

$$I = Y = 0.2126 \cdot R + 0.7152 \cdot G + 0.0722 \cdot B \tag{3.2}$$

One can extract the intensity-time curve by calculating I for all pixels in a designated region of interest (ROI) and determining the mean value at each timeframe.

While executing the work described in this thesis, two different strategies for the extraction of quantified inflow parameters were employed. The first entails an objective and automated approach of determining inflow-based parameters that have previously been studied and reported in literature. In the second strategy, a new set of parameters is introduced.

3.2 Changepoint detection

Previous research on FA quantification investigated various parameters that depend on designating the start-and endpoint of intensity increase (T_0 and T_{max}). Several of these parameters are illustrated in Figure 3.1.[1] Retrospective studies found that for example $T_{1/2}$ (time to reach half of the maximal intensity) had considerable predictive value with regard to anastomotic leakage in colorectal surgery. However, inflow-based parameters like $T_{1/2}$ are less straightforward to extract from measured signals than intensity-based parameters. Previous studies have therefore employed the manual extraction of these parameters. In addition to being

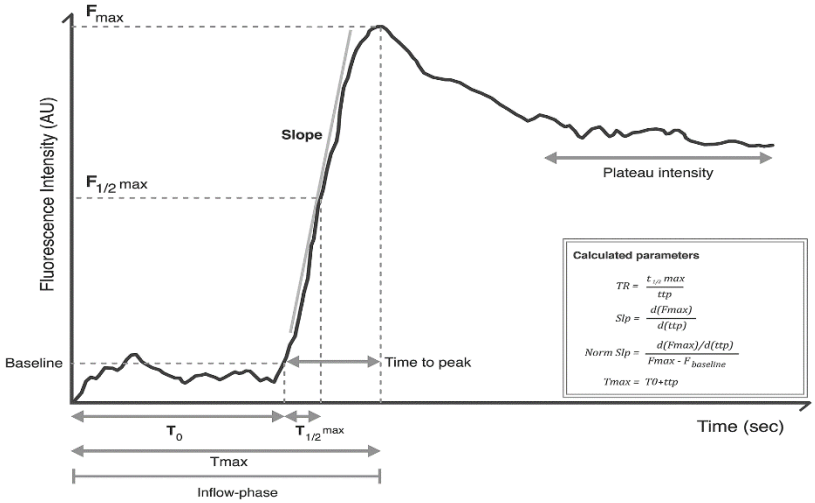

Figure 3.1. *Example of an intensity-time signal of FA. Several quantifiable parameters are defined.[1]*

subjective, this approach is time-consuming and not suitable for an intraoperative workflow. For this reason, a changepoint detection method was developed that appoints T_0 and T_{max} semi-automatically. Appendix A contains the supplementary material of the manuscript in Chapter 5, where this algorithm is discussed in detail.

The study presented in Chapter 5 itself discusses the external validation of the algorithm, along with automated $T_{1/2}$ calculation in 32 patients without impaired intestinal perfusion. The findings show that the algorithm is often successful in assigning T_0 and T_{max}, making it a promising tool for future research on previously defined inflow parameters.
However, since the ambiguity in assigning T_0 and T_{max} (as illustrated in Figure A.2) increases in case of impaired perfusion, the strength of the algorithm lessens. Moreover, the relative complexity of the algorithm prohibits the use of *optimized vector calculations*. This means that ROI's must be analysed in succession, which severely increases the computational cost. Parametric mapping, which entails the creation of a heatmap based on (inflow) parameters, requires analysis of many small ROI's and is therefore unfeasible using the aforementioned approach. The desire to develop an on-site FA quantification tool, that provides direct integration of inflow parameters with live footage, motivated the decision to abandon the parameters established in previous literature. Instead, new parameters were defined while keeping factors like computational efficiency and risk of ambiguity in mind.

3.3 Novel quantification method

3.3.1 Parameter definition

Two new parameters with accompanying calculation algorithms were defined. Time to peak (TTP) was specified as the time between reaching 20% and 80% of the total intensity increase. Normalized peak slope (NPS) represented the maximum slope of a curve-fitting of the signal, normalized with respect to the total intensity increase.

3.3.2 Filtering and calculations

We consider equidistantly sampled intensity-time curve $I(t)$, within a window with size n + 1, centred around sample k.

$$\left(I_{k-n/2}, \dots, I_k, \dots\ I_{k+n/2}\right)$$

The data samples in this window can be approximated by a first order polynomial (i.e. a line; see left panel of Figure 3.2), defined by two polynomial descriptors c_1 and c_0:

$$I = c_1 t + c_0 \tag{3.3}$$

Eq. (3.3) can be drawn for each sample in the window, resulting in a set of linear equations:

$$\begin{bmatrix} k - n/2 & 1 \\ \vdots & \vdots \\ k + n/2 & 1 \end{bmatrix} \begin{bmatrix} c_1 \\ c_0 \end{bmatrix} = \begin{bmatrix} I_{k-n/2} \\ \vdots \\ I_{k+n/2} \end{bmatrix} \tag{3.4}$$

Shortly denoted as:

$$A\boldsymbol{x} = b \tag{3.5}$$

If we aim to find $\boldsymbol{x}$ (c_0 and c_1), we need to find a solution for the inverse of A, denoted as $(A^{-1})^*$. This is done numerically with a least-squares approximation according to:

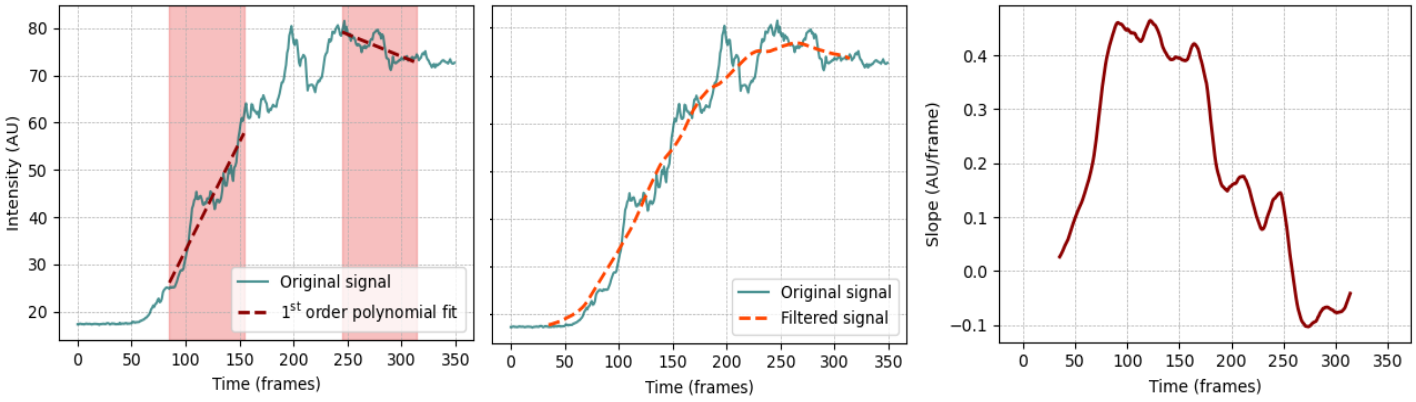

Figure 3.2. *Example of the introduced filtering and slope approximation technique with a window size of 70 frames.* ***Left:*** *First order polynomial fitting at* $k = 120$ *and* $k = 280$. ***Middle:*** *Result of moving average filter (polynomial descriptor* c_0*).* ***Right:*** *Slope approximation (polynomial descriptor* c_1*).*

$$(A^{-1})^* = \min_B \|AB - I\|_2^2 \tag{3.6}$$

where I is the identity matrix. Polynomial descriptors c_0 and c_1 can subsequently be calculated using:

$$\boldsymbol{x} = (A^{-1})^* \cdot b \tag{3.7}$$

Since only the window size is required to evaluate Eq. (3.6), $\boldsymbol{x}$ can be determined for all possible window locations k by directly putting the measured intensity values in b and evaluating Eq. (3.7).

Accordingly, we can move the window and find the slope of the fitted polynomial (which is c_1) at all possible values of k by performing a discrete convolution of $I(t)$ with the reversed first row of $(A^{-1})^*$ as kernel. Evaluating c_0, which in essence means the application of a moving average filter, can be performed by employing the reversed second row of $(A^{-1})^*$ as convolution kernel. The reversed first and second row of $(A^{-1})^*$ are denoted as $\boldsymbol{z_1}$and $\boldsymbol{z_2}$ respectively. In this approach, $\boldsymbol{z_1}$and $\boldsymbol{z_2}$ act as the coefficients of a finite impulse response (FIR) filter. So, a filtered version of $I(t)$ can be achieved with convolution:

$$\hat{I}(t) = I(t) * \boldsymbol{z_1} \tag{3.8}$$

And the slope approximation with convolution:

$$I'(t) = I(t) * \boldsymbol{z_2} \tag{3.9}$$

The effects that are achieved by performing these operations are demonstrated in the middle and right panel of Figure 3.2.

For the calculation of TTP, the baseline and peak intensity ($I_{0\%}$ and $I_{100\%}$) are determined at first by calculating the median of respectively the ten lowest and highest values in the signal. Thereafter, the intensity levels at 20% and 80% of the total increase are determined according to:

$$I_{20\%} = I_{0\%} + 0.2 \cdot (I_{100\%} - I_{0\%}) \tag{3.10}$$

$$I_{80\%} = I_{0\%} + 0.8 \cdot (I_{100\%} - I_{0\%}) \tag{3.11}$$

The moment of reaching these intensity levels is searched for in $\hat{I}(t)$.

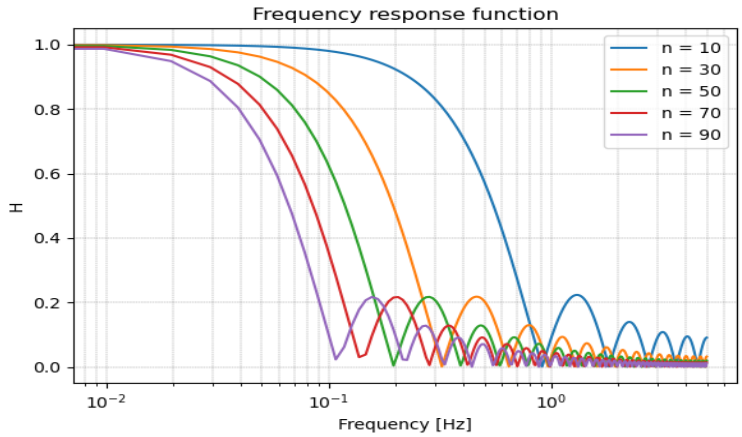

Figure 3.3. *Frequency response function of a moving average filter with various window sizes.*

NPS is calculated by finding the maximal value of the approximated slope signal and subsequent normalization and conversion to units [%/second] by:

$$NPS = \frac{max(I'(t))}{I_{100\%} - I_{0\%}} \cdot 10 \cdot 100\% \tag{3.12}$$

The effects of the FIR filter can be tweaked by altering the window size n. Fitting the line in a wider window suppresses the effects of short 'bumps' in the signal, and thus results in stronger smoothing. Figure 3.3 shows the frequency response curve of a moving average filter for various window sizes. These curves explain the smoothing effect in the frequency domain: the range of frequencies that passes through the filter shifts to the lower end of the spectrum with increasing window size. It should be noted that this filtering method performs very poor as low-pass filter in the frequency domain, due to the long roll-off and unsatisfactory stop-band attenuation. However, its smoothing capabilities in the time-domain and computational efficiency make it greatly suited for our application. It is, nonetheless, crucial to select an appropriate window size. Figure 3.4 displays the effects of a small and large n. At n=100, the steep intensity increase in 3.4B is diminished by the filtering effects, which would result in underestimation of the peak slope. A window size of 20 preserves the increase, and thus the proper peak slope (3.4A). Naturally, steeper slopes require a smaller n to remain intact. At the same time, n=20 also preserves signal deviations due to artefacts (3.4C), thereby overestimating the slope, while n=100 would provide the desired slope value in Figure 3.4D.

In summary, the window size must selected in such a way that:

- Artefacts and high frequent noise are not the underlying factor of an observed slope value, or the cause of premature reaching of the $I_{20\%}$ or $I_{80\%}$ level.
- Steep intensity increases, that are found in case of healthy perfusion, are flattened as little as possible, so the power in discriminating healthy and impaired perfusion remains.

Likewise, the limits of 20% and 80% in calculating TTP are arbitrary but important choices. When selected close to 0% and 100%, the algorithm becomes more sensitive to errors and ambiguities resulting from plateaus and artefacts. On the contrary, setting the limits to close together weakens the discrimination between healthy and impaired perfusion.

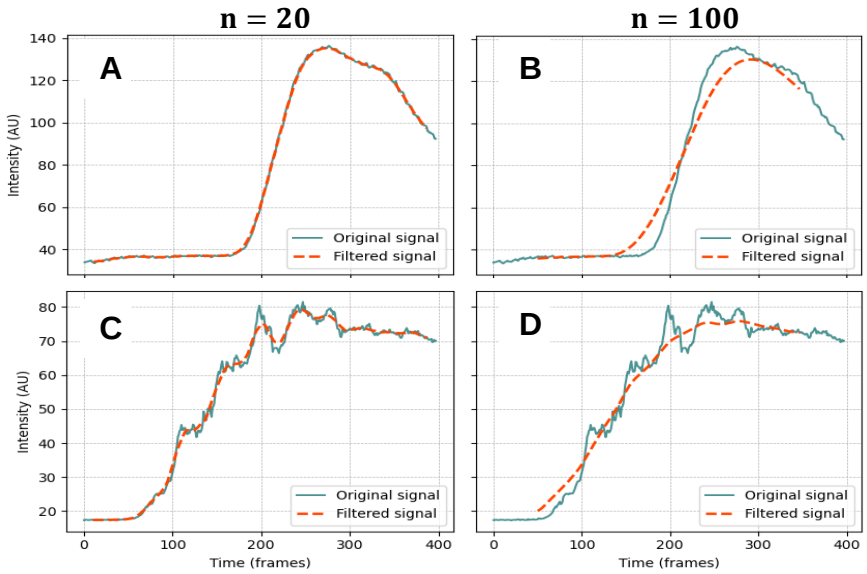

Figure 3.4. *Filtering effects of window sizes n=20 and n=100, illustrated for a rapidly increasing low-noise signal (**A/B**) and a slower increasing signal with high frequent noise and movement artefacts (**C/D**). Note the steeper peak slopes in the filtered signal in **A** and **C**, compared with **B** and **D**. Figure **B** illustrates underestimation of the intensity increase and figure **C** illustrates over-estimation of the desired slope due to artefacts.*

Based on trial and error when employing a clinical dataset of measurements in patients with and without suspected perfusion impairment (described in Chap. 5 and Chap. 6), filtering with n=40 and limits of 20% and 80% were deemed appropriate for determining TTP. In the calculation of NPS, the differentiating filter required n=75 to achieve the desired results.

3.4 Software

Interactive software tools for the off-site and on-site analysis of FA images were developed in Python 3.7 (Python Software Foundation, Wilmington, DE, USA). On-site analysis is facilitated by propagating RGB-frames of the NIR imaging system through an HDMI frame grabber into a personal computer. Off-site analysis is based on intraoperative MP4 recordings.

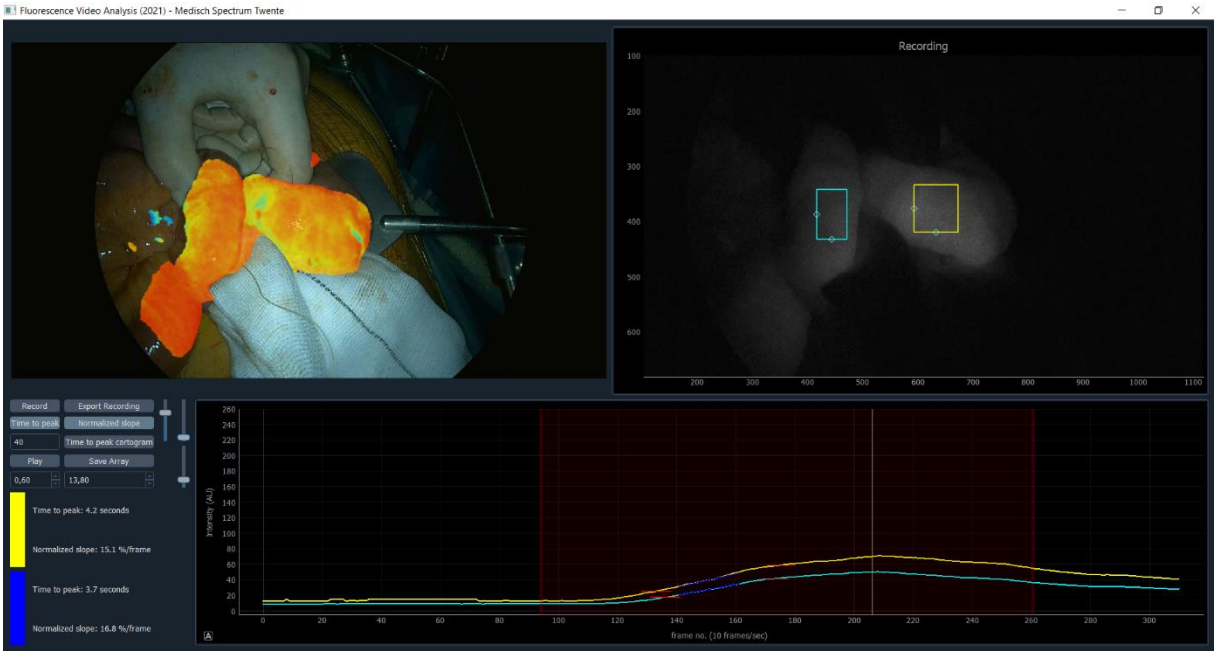

Figure 3.5. *Software tool for intraoperative quantification of live FA data. The left panel shows live video footage from the imaging system with an integrated TTP heatmap that is based on intraoperatively recorded FA data, which can be analysed using the right panel and the bottom graph. Several controls are implemented to adjust window size, transparency of the heatmap etc.*

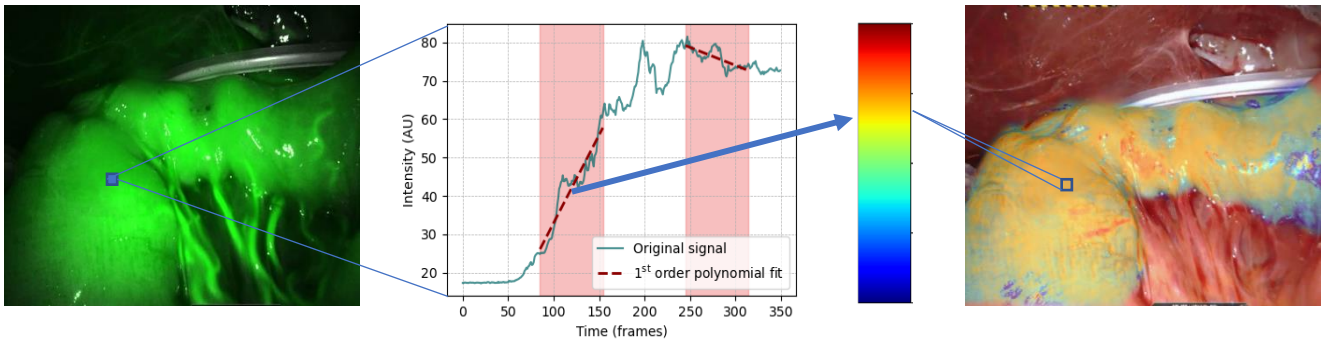

Figure 3.6. *Schematic overview of the parametric mapping process, where a colour is assigned to each pixel based on a quantified inflow-parameter and subsequently overlayed onto live white-light footage.*

For on-site analysis, the user interface consists of two image panels and one window for analysis of intensity signals (see Fig. 3.5). Live video footage is continuously displayed on panel 1, while panel 2 is reserved for analysis of FA images. The FA data is collected by recording live video, started after ICG is injected in the bloodstream, and converting to intensity values according to Eq. (3.1) and (3.2). This data is contained in a three-dimensional array. The user can review the FA data visually and perform quantified analysis in two ROI's simultaneously. TTP and NPS are calculated automatically when the ROI is moved. Moreover, parametric mapping (see Fig. 3.6.) of TTP and NPS is possible with the assistance of optimized multidimensional data processing algorithms (Python *SciPy* library) to perform the convolutions in Eq. (3.8) and Eq. (3.9) for all pixels simultaneously. Parameters can be displayed as a heatmap over both image panels. If the imaging system is switched into regular white light modus, FA quantification can be integrated in the live operating footage. Two semi-automatic approaches are incorporated in the software to enable segmentation of the heatmap.

References

1. Lütken CD, Achiam MP, Svendsen MB, Boni L, Nerup N. Optimizing quantitative fluorescence angiography for visceral perfusion assessment. Surg Endosc. 2020;34(12):5223-5233.

4 In Vitro Evaluation of Near-infrared Imaging System Behaviour

4.1 Introduction

4.1.1 Background: ICG radiometry

We consider a surface A containing ICG molecules (see Fig. 4.1). Photons emitted by these molecules form a radiant flux Φ_A $[W]$. Consequentially, the surface has a brightness that can be registered by a camera sensor, called the surface radiance L_A $[Wsr^{-1}m^{-2}]$. Radiance is defined as the radiant flux emitted by the surface per unit solid angle per unit foreshortened area. Solid angle ω measures the range of directions that photons can travel while being captured by the camera lens, while foreshortened area describes the area of the surface that is 'seen' by the camera sensor (or pixel). The radiant flux that falls on the sensor, per unit area of the sensor, is the camera irradiance E_C $[Wm^{-2}]$. This property is directly related to L_A. A CCD or CMOS chip eventually transforms the measured irradiance E_c into pixel intensities.

The *distance* between sensor and surface has no effect on the measured radiance (if the effects of scattering and absorption in air are not considered). When the sensor is moved away from the surface A, the solid angle subtended from a point on A by the camera lens decreases, causing the sensor to receive less radiant flux from that point (inverse-square law effect). However, the total surface area that is captured by the sensor (on the same pixel) also increases, cancelling out the aforementioned effect. Since the surface radiates light in all directions, Lambert's cosine law can be applied. This means that the radiant intensity is proportional to the cosine of the angle θ between the line of sight and the surface normal of A, and thus falls off when the surface is observed from an angle. However, the apparent area that supplies this intensity also falls off with cosine of θ, causing the surface radiance to be unaffected by *viewing direction*.

Considering the above, one could state that moving a NIR camera optic away or at a different angle from a sample containing ICG molecules should have no impact on the obtained intensity values. This is, however, untrue. Before ICG molecules will emit photons, electrons need to be excited by means of photoexcitation. The light source that facilitates this excitation is integrated in the camera optic, meaning it moves together with the sensor. By approximation, this source can be considered as a point source. This means that increased distance results in decreased light intensity, according to the inverse-square law, but does not result in an increased light-emitting area. The light intensity falling on the surface also falls off proportional to the cosine of the viewing angle. Accordingly, increased distance and viewing angle suppress the excitation of ICG-electrons and subsequently the fluorescent flux from the surface.

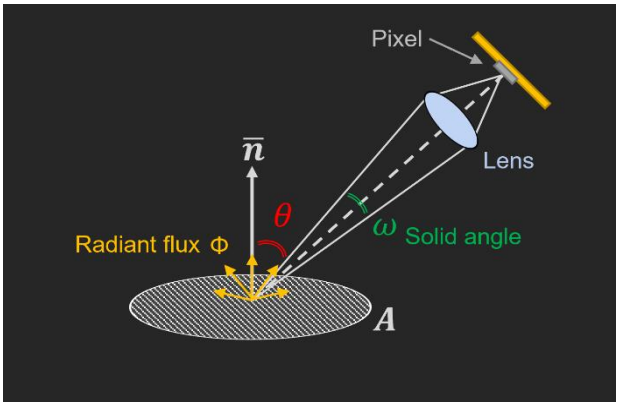

Figure 4.1. *A surface that emits radiant flux Φ, measured by a camera sensor. Solid angle ω defines the range of light directions that is captured by the lens. The angle between the surface normal* $\overline{\boldsymbol{n}}$ *and the orientation of the sensor is denoted as θ.*

In any form of (quantified) fluorescence imaging, one aims to gain information on the presence of a fluorescent dye (e.g. ICG) at a certain location and point in time. The best indicator of this information is the surface radiance, which is linearly mapped to irradiance of the camera sensor. However, final image data is generated by the camera electronics. A camera response function describes how values of irradiance are eventually translated to pixel values. It depends on technical properties like exposure time, but also on digital data processing. A linear, invariant camera response function is ideal for quantification. This means that intensity-time curves are merely scaled as a result of changes in measurement system and circumstances, and that the dynamics remain the same. Inflow-based parameters are thus unaffected. Moreover, intensity measurements between various systems could be compared after correction with a single known constant.

4.1.2 Aim and hypotheses

A wide variety of commercial and non-commercial NIR imaging systems are available. Two of these are present in Medisch Spectrum Twente, both integrated as a module in a system for laparoscopic surgery. In order to perform fluorescence-guided surgery, the behaviour and comparability of both systems should be known. This is especially important when objective, quantitative decision-making is pursued. Under the assumption that increased ICG presence results in higher radiant flux, it is desirable that a surface with high radiant flux is portrayed with a higher pixel intensity on an imaging system. In this study, static and dynamic phantom experiments are conducted to evaluate the behaviour of digital NIR imaging systems in MST with regard to ICG concentration, measurement circumstances and perfusion dynamics.

It was expected that, within the dynamic range of the camera system, distance would have an inverse quadratic effect on pixel intensity. Moreover, it was expected that increasing ICG concentration would increase pixel intensity until a peak is reached when self-quenching of the light by ICG molecules is dominant.[1]

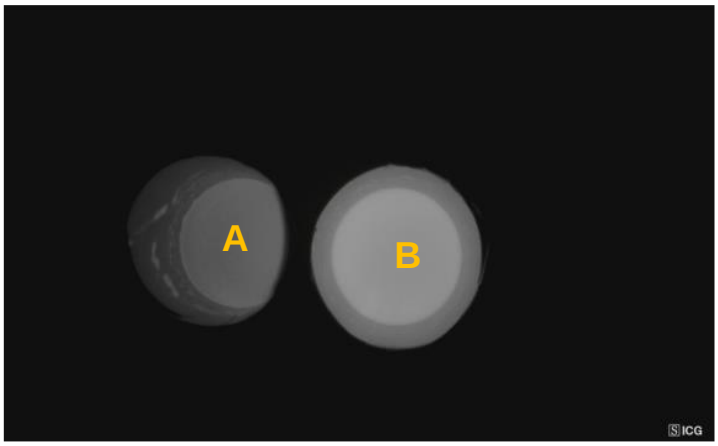

Figure 4.2. *Static experiment setup captured on the Storz system in monochromatic NIR mode.* ***(A)*** *Reference sample with consistent concentration of 0.31 µM.* ***(B)*** *Test sample with varying concentration.*

4.2 Materials & Methods

During all experiments, NIR image acquisition by the DaVinci X and Storz systems was performed simultaneously, while approximating a line of sight perpendicular to the surface of the sample. Quantification analysis was performed using in-house developed software, where parameters TTP and NPS were extracted according to Chapter 3.

4.2.1 Static experiments

ICG was prepared according to clinical protocol (5 mg/ml) and diluted in long-life milk. All concentrations were obtained by dilution of the same solution. Samples were measured consecutively, but images were captured in one MP4 recording. All measurements were conducted at a sample-optic distance of 5, 10, 15 20 and 25 cm.

To investigate a varying camera response function, the same dilutions were measured at 20 and 25 cm next to a reference sample with a consistent concentration of 0.31 µM (see Fig. 4.2).

4.2.2 Dynamic experiments

For the purpose of measuring ICG dynamics, a basic perfusion phantom was implemented in an open flow system. This phantom consisted of a tube branching out into four parallel routes and subsequently a sponge, representing capillary circulation. Long-life milk was pumped through the phantom and into a container at a consistent flow. A separate contrast-pump, containing a 10 µM ICG solution in milk, was connected to the afferent tube (see Fig. 4.3) and facilitated the simulation of an ICG bolus. Size of the bolus was set to 5 ml in all experiments. Measurements were conducted with a distance of 15 or 22 cm, ICG bolus inflow rate of 2.5 or 5 ml/s and milk flow of 11 or 22.5 ml/s, contributing to a total of eight. Intraclass correlations (ICC) were calculated according to the two-way mixed single score model and presented with a 95% confidence interval.

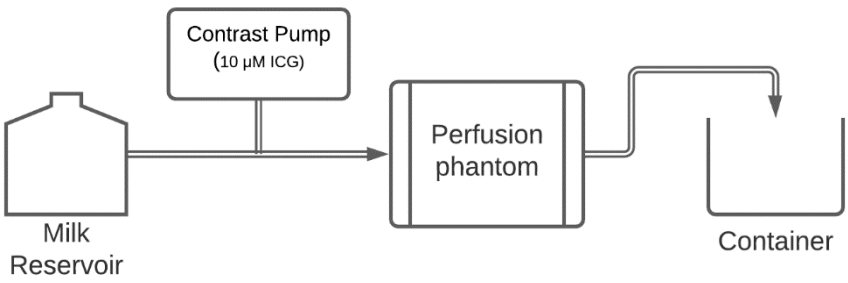

Figure 4.3. *Schematic diagram of a flow system as used in the dynamic experiments.*

4.3 Results

4.3.1 Static experiments

Figure 4.4 shows the intensity levels that represent various ICG concentration levels for both systems. On the DaVinci system, it is noticeable that, in the investigated range of concentrations, a higher concentration yields higher intensity values (following a logarithmic trend) until the dynamic range is reached. In addition, a greater sample-optic distance decreases the measured intensity. Conversely, the Storz system displays higher intensities when distance in increased. None of the systems displayed clear signs of dominant self-quenching in this concentration range.

In Figure 4.5, the effects of neighbouring ICG radiance on measured intensity values are illustrated. In the DaVinci system, the intensity of the reference sample remains unaffected by the varying concentration next to it. On the contrary, it can be observed that in the Storz system the intensity of the reference sample decreases with increasing intensity of the test sample. Note that this effect stops when maximal intensity is reached in the test-sample, regardless of further increase in concentration.

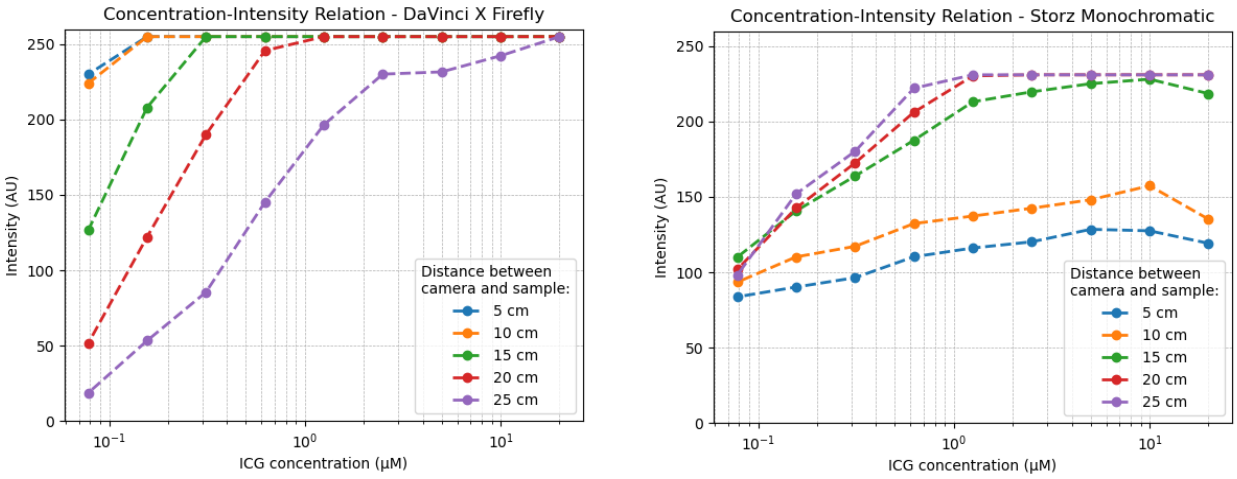

Figure 4.4. *Intensity values of ICG solutions with various concentrations on the DaVinci X Firefly (**left**) and Storz Monochromatic NIR (**right**) system.*

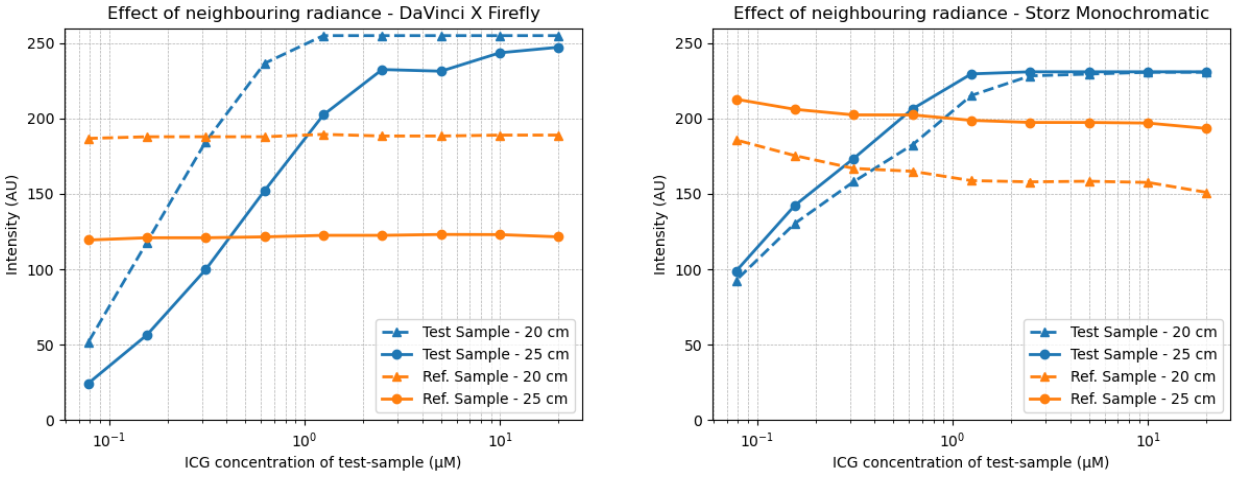

Figure 4.5. *Intensity values of a test-sample with varying ICG concentration and a neighbouring reference sample with an ICG concentration of 0.31 μM on the DaVinci X Firefly (**left**) and Storz Monochromatic NIR (**right**) system.*

Table 4.1. Inflow Quantification Results of Dynamic Experiments.

Distance (cm)	Milk flow (ml/s)	ICG inflow (ml/s)	TTP (seconds)		NPS (%/second)	
			DaVinci	Storz	DaVinci	Storz
15	11	2.5	3.5	5.9	15.5	11.3
		5.0	3.3	4.3	16.1	13.7
	22.5	2.5	2.2	2.5	19.2	18.0
		5.0	2.1	2.5	19.3	17.4
22	11	2.5	3.8	4.3	14.6	13.6
		5.0	3.5	4.7	15.8	13.4
	22.5	2.5	2.5	2.2	18.6	18.4
		5.0	2.1	2.5	19.3	18.7

4.3.2 Dynamic experiments

The results of signal quantification in all eight measurements are depicted in Table 4.1. Figure 4.6 illustrates the comparison of inflow parameters between both systems. Higher milk flow resulted in lower TTP and higher NPS for both systems. Increased ICG injection flow gave similar effects in the DaVinci system, but not in the Storz system. Generally, distance between optic and phantom had no clear effect on the inflow quantification. The measurements in both systems had an overall ICC of 0.72 (95% CI: 0.11 – 0.94) for TTP and overall ICC of 0.86 (95% CI: 0.47 – 0.97) for NPS.

The largest discrepancy between the systems was found in the measurement with milk flow of 11 ml/s and ICG-solution inflow of 2.5 ml/s at a distance of 15 cm. This measurement is outlined in Figure 4.7, along with its equivalent at 22 cm. Next to the intensity-time curves for each system, the DaVinci signal is scaled such that its peak intensity conforms with the Storz signal. This way, the dynamic ('time-based') properties of both signals can be compared. The scaled DaVinci signal is notably more similar to the Storz signal at 22 cm.

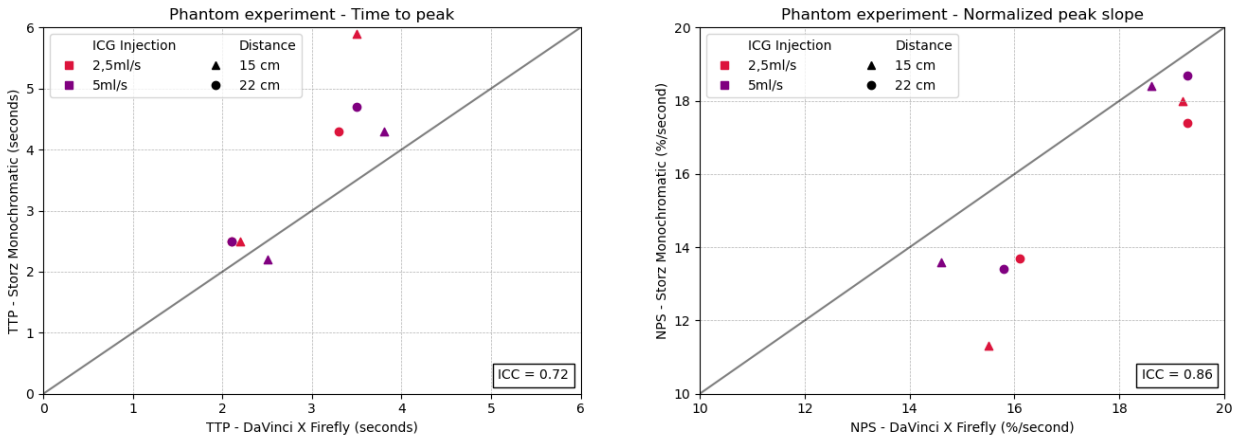

Figure 4.6. *Scatterplots representing inflow parameters TTP (**left**) and NPS (**right**) for all measurements, as acquired by both NIR imaging systems.*

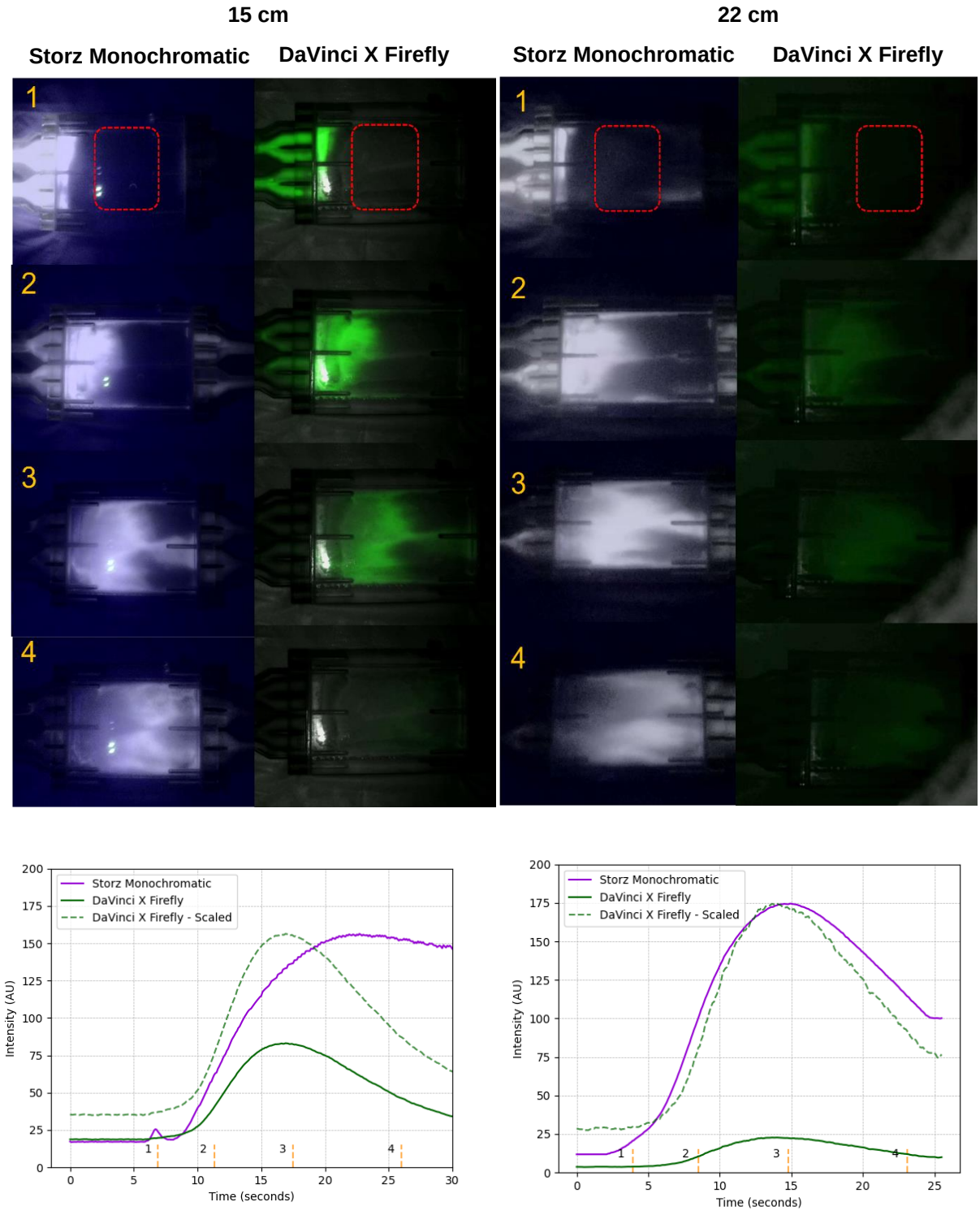

Figure 4.7. *Dynamic perfusion phantom with milk flow of 11 ml/s and ICG inflow of 2.5 ml/s, measured at 15 cm (**left** panel) and 22 cm (**right** panel). Frames are displayed of **(1)** inflow in afferent tubes, **(2)** first inflow in ROI (red box), **(3)** maximal intensity in ROI and **(4)** during outflow in ROI. Graphs display the intensity-time curves, measured in the ROI. The dotted green line represents the signal measured using the DaVinci system, scaled with a factor such that the peak intensity is equal with that of the Storz system's curve.*

4.4 Discussion

Reliable and quantitative fluorescence-guided surgery requires knowledge on the behaviour of employed imaging systems. In this study, we conducted static and dynamic experiments to investigate how the two NIR imaging systems in MST react to various ICG concentrations and measurement circumstances, and how data from these systems can be compared.

Static experiments revealed that the DaVinci system displays various concentrations as expected. Within the dynamic range of the camera, higher concentrations and a closer distance result in higher intensities. Moreover, the presence of a neighbouring radiant source does not influence intensity values, indicating an invariant camera response function. In Figure 4.4, it can be seen that measurements within the dynamic range of the DaVinci system approximate the expected inverse quadratic relation between distance and intensity. In contrast, the Storz system shows rather unpredictable behaviour. Although larger ICG concentrations are generally displayed with higher intensity values, a closer proximity of the optic to the sample generated lower intensity. This effect was amplified in the step between 10 and 15 cm. There is no known explicit explanation for this finding. It can, however, be presumed that a certain degree of non-linear processing precedes the final image. The variation of this processing is illustrated by the inconsistent rendering of an unaltered ICG-sample, as displayed in Figure 4.5.

It became apparent that the rendering of images in the Storz system typically resulted in higher TTP and lower NPS values, compared with the DaVinci system. The most evident example was the measurement with low milk flow and low ICG inflow at 15 cm (see Fig. 4.7). Although the DaVinci system displays the fluorescence with lower intensities, the *dynamics* of the curves should be the same when the systems observe the same experiment. However, linear upscaling of the DaVinci signal demonstrates the considerable differences between the two signals that subsequently result in different TTP and NPS values. Note, for example, that the outflow of ICG is not portrayed by the Storz system in the same way as by the DaVinci system. Interestingly, the notable discrepancies are diminished when the measurement is repeated at a larger distance. Both systems show similar *dynamics*, exemplified by similarity between the Storz curve and scaled DaVinci curve. An explanation for this can be found in the active 'scaling' processes in the Storz system, as observed in the static experiments. These are most probably triggered by the sudden exposure to large amounts of NIR radiance, especially in the afferent tubing of the phantom (see Fig. 4.7, frame 1). Naturally, this variable processing influences the course of the intensity values, and thus the inflow-based quantification. Moving the optic away from the phantom decreases the radiant intensity that the system is exposed to, and thereby reduces the unpredictable scaling effects. Inflow parameters are more reliable as a result.

Although 15 cm is a realistic optic-tissue distance for *in vivo* measurements, the effects as seen in the aforementioned example are not expected to be as drastic in patient studies. The sudden exposure to high intensities was caused by the transparent tubing and is unlikely to occur *in vivo*, due to substantial light absorption by tissue. Inflow-based parameters are therefore, within the studied range of flows and distances, reasonably comparable between the two systems. This level of comparability is considered to be sufficient for proof-of-concept studies. However, since an invariant linear camera response function cannot be guaranteed, it is strongly advised to perform analysis on 'raw data' of the NIR sensor when conducting clinical studies in the pursuit of reliable threshold values. This is especially true for the Storz system. If thresholds for intensity values are

desired, for example in fluorescence-guided oncologic surgery, use of the Storz system without access to raw data is not advised.

References

1. Yuan B, Chen N, Zhu Q. Emission and absorption properties of indocyanine green in Intralipid solution. J Biomed Opt. 2004;9(3):497.

5 Fluorescence-Based Quantification of Gastrointestinal Perfusion: A Step Towards an Automated Approach

H.G.M. Vaassen BSc,[a] B. Wermelink MSc,[a, b] R.H. Geelkerken, Prof., MD, PhD,[a, b] and D.J. Lips, MD, PhD[c]

[a] Multi-Modality Medical Imaging (M3i) group, TechMed Centre, University of Twente, Enschede, The Netherlands
[b] Section Vascular Surgery and [c] section Gastrointestinal and Oncology Surgery, Department of Surgery, Medisch Spectrum Twente, Enschede, The Netherlands

Published in Journal of Laparoendoscopic & Advanced Surgical Techniques – March 2021 – Online ahead of print

Abstract

Background – Qualitative fluorescence angiography (FA) provides insights in intestinal tissue perfusion, but today it is not yet accurate in predicting anastomotic leakage. In order to improve peroperative detection of impaired perfusion, quantified parameters should be investigated using a standardised method. The aim of this study was to develop a (semi) automated algorithm for comprehensive and convenient analysis of FA parameters.

Materials and Methods – An analysis tool was developed for the extraction of quantified FA parameters. The start- and endpoint of intensity increase (T_0 and T_{max}) were automatically detected in the intensity-time curves. Algorithm performance was measured against manual assignment of T_0 and T_{max} by nine independent observers in 18 in vivo generated test signals, using the Intraclass Correlation Coefficient (ICC). Characteristics of parameter $T_{1/2}$ (time to 50% of maximal intensity) were analysed in normally perfused small intestine of 32 subjects who underwent robotic laparoscopic surgery.

Results – Automated detection of T_0 and T_{max} was successful in all subjects. Output of the algorithm had an excellent agreement with the median of the human observations: ICC = 0.95 (95% CI: 0.86 – 0.96). Overall, $T_{1/2}$ had a median value of 5.1 (IQR = 2.4) seconds and a minimal and maximal value of 1.3 and 9.9 seconds respectively.

Conclusions – The presented method provided convenient data analysis in the search for effective FA quantification. Future research should expand the data to find adequate threshold values for peroperatively identifying insufficient perfusion and investigate the influence of physiological conditions.

5.1 Introduction

Inadequate local or systemic perfusion is regarded as a substantial factor in complications after gastrointestinal surgery. The most feared and frequent example is anastomotic leakage (AL), associated with strongly increased morbidity and mortality and incidence rates varying from 3 to 19%.[1–4] In current practice, blood supply is evaluated peroperatively by means of clinical observations such as mucosal colour, palpable pulsations and bleeding from the marginal artery. However, these methods lack accuracy and objectivity, irrespective of a surgeon's experience.[5] Alternative approaches including the use of Doppler, laser speckle contrast imaging and hyperspectral imaging have yet failed to reach clinical implementation, since no recommendation can be made regarding their applicability due to technical difficulties and low reproducibility.[6–10] There is a need for objective and reliable peroperative detection of insufficient intestinal perfusion.

In recent years, fluorescence angiography (FA) has emerged as a promising tool for yielding intraoperative insight in local perfusion dynamics. FA involves the intravenous injection of contrast agent indocyanine green (ICG) and subsequent monitoring of its fluorescent appearance in bowel tissue. The role of FA in peroperative decision-making during colorectal surgery has already been demonstrated.[6,11–13] Furthermore, superiority of FA over judgement on clinical signs alone in the detection of perfusion impairment has been shown in experimental models.[14,15] However, the acquired images are evaluated in a qualitative fashion, making them sensitive to misinterpretation. In addition, multicentre randomized controlled trials failed to show a significant reduction in anastomotic leakage after peroperative implementation of FA.[12,13,16] It becomes apparent that the current qualitative interpretation of FA is unreliable, creating the need for more objective quantification.[16,17]

Animal studies showed a great ability of quantified parameters to indicate blood flow and tissue ischemia.[14,18] Quantification should be based on reproducible signal properties, meaning that circumstances other than tissue perfusion should not be influential. For this reason, the use of intensity-based parameters such as maximal intensity is not advised, since these depend on factors like ICG dosing and the distance between tissue and camera. Time-based dynamics of the signal are more consistent. Parameter $T_{1/2}$, defined as the time between first intensity increase and the point of reaching 50% of the maximal intensity, showed promising predictive value for AL in colorectal surgery.[7,19] However, as of yet there is no general consensus on the interpretation of quantified FA.[16,20] Additional data obtained using a standardised method is required to distinguish normal and pathological findings.

This study presents a convenient and objective semi-automated method for the acquisition of peroperative quantitative parameters in FA. Moreover, as a first step towards a differentiating threshold value, the characteristics of the parameter $T_{1/2}$ in normally perfused small intestine are investigated.

Table 5.1: Characteristics of Patients Who Underwent Fluorescence Angiography During Robotic Laparoscopic Surgery (n = 32)

Characteristic	Data
Age (years; mean ± SD)	66 ± 12
Gender (%)	
Female	19 (59.4)
Male	13 (40.6)
BMI (kg/m$^{2;}$ mean ± SD)	25.7 ± 5.3
ASA score (%)	
I	4 (12.5)
II	20 (62.5)
III	8 (25.0)
Diagnosis (%)	
Pancreatic malignancy[a]	10 (31.3)
Colorectal liver metastases	6 (18.8)
Cholangiocarcinoma	4 (12.5)
Duodenum carcinoma	3 (9.4)
Cholecystolithiasis	3 (9.4)
Colon cancer	2 (6.3)
Other	4 (12.5)
Vascular risk factors (%)	
Smoking (>5 cigarettes/day)	7 (24.1)
Hypertension	5 (16.1)
Coronary disease	4 (13.8)
Diabetes	3 (9.4)
Vascular disease	2 (6.7)

[a]Includes intraductal papillary mucinous neoplasms.
ASA, American Society of Anaesthesia; *BMI*, body mass index; *SD*, standard deviation.

5.2 Materials and Methods

5.2.1 Data acquisition

A total of 33 patients who underwent robotic laparoscopic abdominal surgery were prospectively included in this study. No ethical approval was needed under the Dutch law on Medical Research on Human subjects, and the need for informed consent was therefore waived. All procedures were performed by one surgeon in Medisch Spectrum Twente (MST) Hospital (Enschede). No patient presented clinical signs suggesting impaired intestinal perfusion. Patient characteristics including laparoscopy indication are presented in Table 5.1. In each patient, FA was performed on the small intestine as a minor extension to standard peroperative FA application. No clinical decisions were made based on the intestinal FA analysis. All FA recordings were obtained using the Firefly module in the Da Vinci X system (Intuitive Surgical, Sunnyvale, CA, USA) after manual intravenous injection of 5 mg ICG (5 mg/ml) and subsequent saline flushing.

5.2.2 Parameter extraction

A software tool for the quantitative analysis of FA recordings was developed in MATLAB R2019a (MathWorks, Natick, MA, USA). The main purpose of this tool was convenient quantification of FA with automated but user-supervised parameter extraction. The algorithm employed several steps. First, an intensity-time curve was determined by calculating the mean value of the green colour channel in a specific region of interest (ROI) for each timeframe. Signal noise was subsequently removed using a lowpass Butterworth filter (2nd order, cut-off frequency = 0.18 Hz). The following

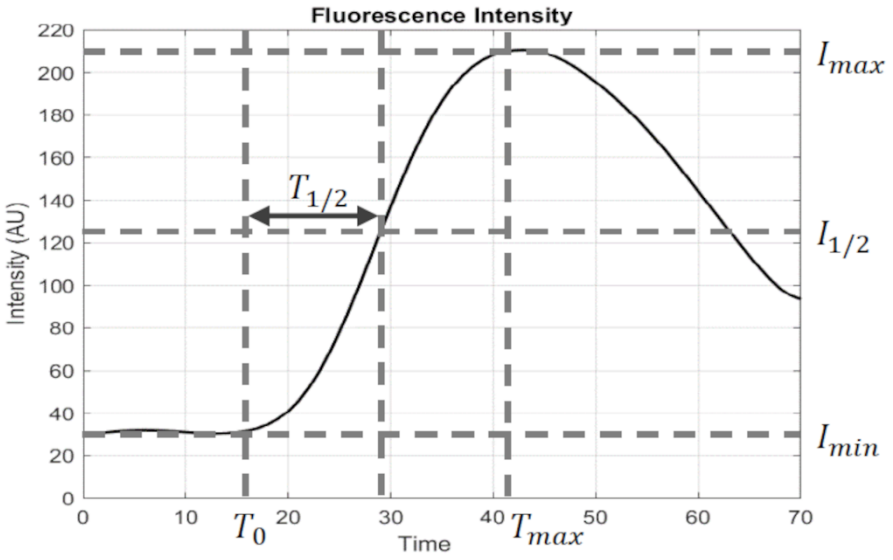

Figure 5.1. *Filtered intensity-time curve of FA. $T_{1/2}$ is defined as the time between first intensity increase and the point of reaching 50% of maximal intensity. FA, fluorescence angiography.*

step was detection of the start- and endpoint of the intensity increase (T_0 and T_{max}; see Figure 5.1). For this purpose, the algorithm searched the intensity curve for points of change in linear trend. This comprised dividing the signal into segments in such a way that the following cost function is minimized:

$$J(m,n) = \sum_{i=m}^{n-1} \left(x_i - \mu([x_m \dots x_{n-1}])\right)^2 - \frac{\left(\sum_{i=m}^{n-1} \left(x_i - \mu([x_m \dots x_{n-1}])\right) * \left(i - \mu([m \dots n-1])\right)\right)^2}{\sum_{i=m}^{n-1} \left(i - \mu([m \dots n-1])\right)^2} \quad (5.1)$$

Where $J(m,n)$ is the residual error, x is the measured intensity in the ROI and m,n index timeframes that divide the segments. After minimization of this expression by varying the segment division, the segment borders are considered changepoints in linear trend.

It is expected that the start- and endpoint of intensity increase are identified as one of these changepoints. Definitive designation of T_0 and T_{max} was performed using multiple conditions based on the slope of the signal. A more detailed description of the processing steps is provided in Appendix A. $T_{1/2}$ was derived directly from T_0 and T_{max}.

The performance of the algorithm in the detection of T_0 and T_{max} was evaluated by measuring its agreement with human observation. Nine independent observers appointed T_0 and T_{max} in a test dataset of 18 signals. The test dataset was generated by measuring the intensity in three random ROI's in the footage of six included patients. As measurement of agreement, the intraclass correlation coefficient (ICC) of the median human input and the algorithm output was computed using SPSS 26.0 (IBM Corp, Armonk, NY). The intra- and inter-observer variability was evaluated using the ICC as well.

5.2.3 Patient analysis

The characteristics of $T_{1/2}$ in patients without impaired perfusion were analysed in a semi-automated fashion. In each recording the small intestine was manually segmented. The segmentation was subsequently divided into smaller polygons according to a 10 × 10 grid (creating multiple ROIs), whereupon $T_{1/2}$ was calculated automatically for each polygon. A

manifold of measurements in each recording allowed for the assessment of patient specific variations in $T_{1/2}$. The characteristics of $T_{1/2}$ were investigated using the five-number summary (i.e. median, minimum, maximum and upper/lower quarters) of all measurements in each patient. Datapoints were considered outliers when they exceeded the 75th percentile plus 1.5 times the interquartile range (IQR) or were inferior to the 25th percentile minus 1.5 times the IQR. In addition, by assigning a colour to each polygon based on the value of $T_{1/2}$, a cartogram was developed for each patient.

5.3 Results

FA was performed on a total of 33 patients, who all had a prosperous postoperative recovery. The recording of one patient was excluded from the analysis of $T_{1/2}$ characteristics, due to faulty ICG admission.

5.3.1 Algorithm performance

Among the nine observers, ICC varied between 0.93 and 0.99 (95% CI: 0.89 – 0.99) for T_0. For T_{max}, intra-observer ICC varied between 0.96 and 1.00 (95% CI: 0.91 – 1.00). The ICC across all observers was 0.95 (95% CI: 0.92 – 0.98) for T_0 and 0.98 (95% CI: 0.96 – 0.99) for T_{max}. Comparison of the algorithm with the median of the human observations provided an ICC of 0.95 (95% CI: 0.86 – 0.96).

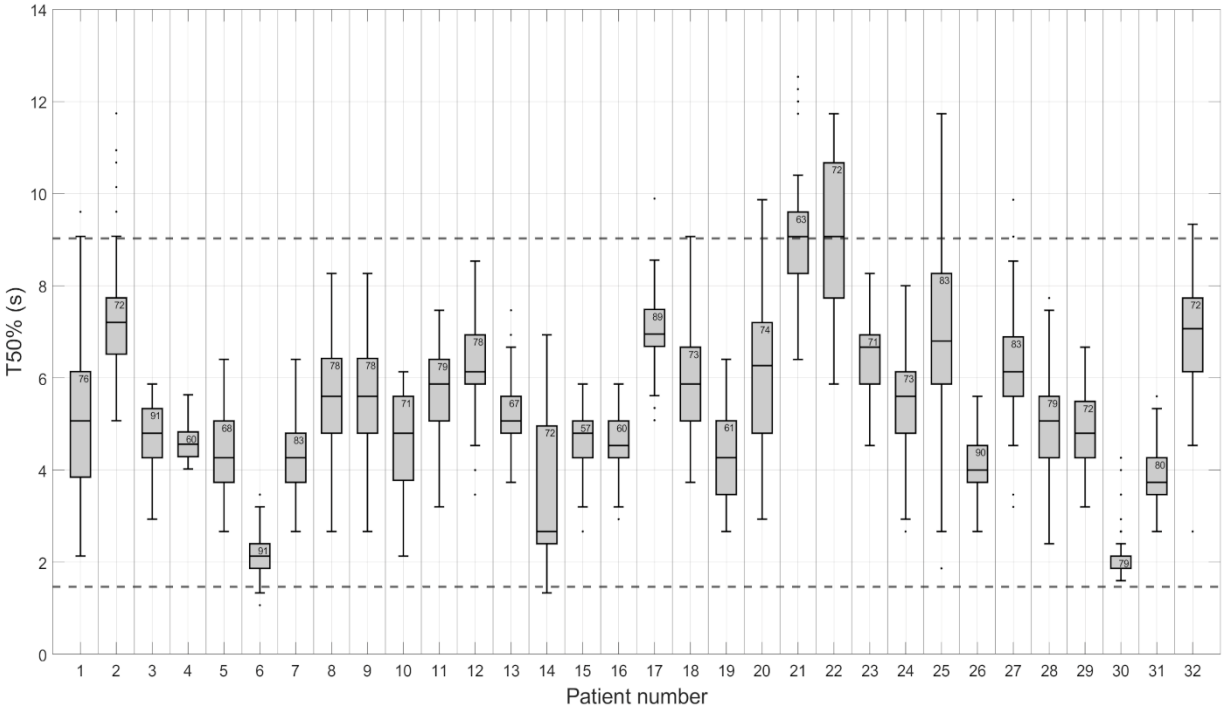

Figure 5.2. *Boxplots representing the measurements of $T_{1/2}$ in the small intestine for all included patients. The total number of ROI's measured in each patient is displayed inside the boxplots. Small dots represent measurements in ROI's that were considered outliers. Dotted lines represent 95% CI for $T_{1/2}$.*

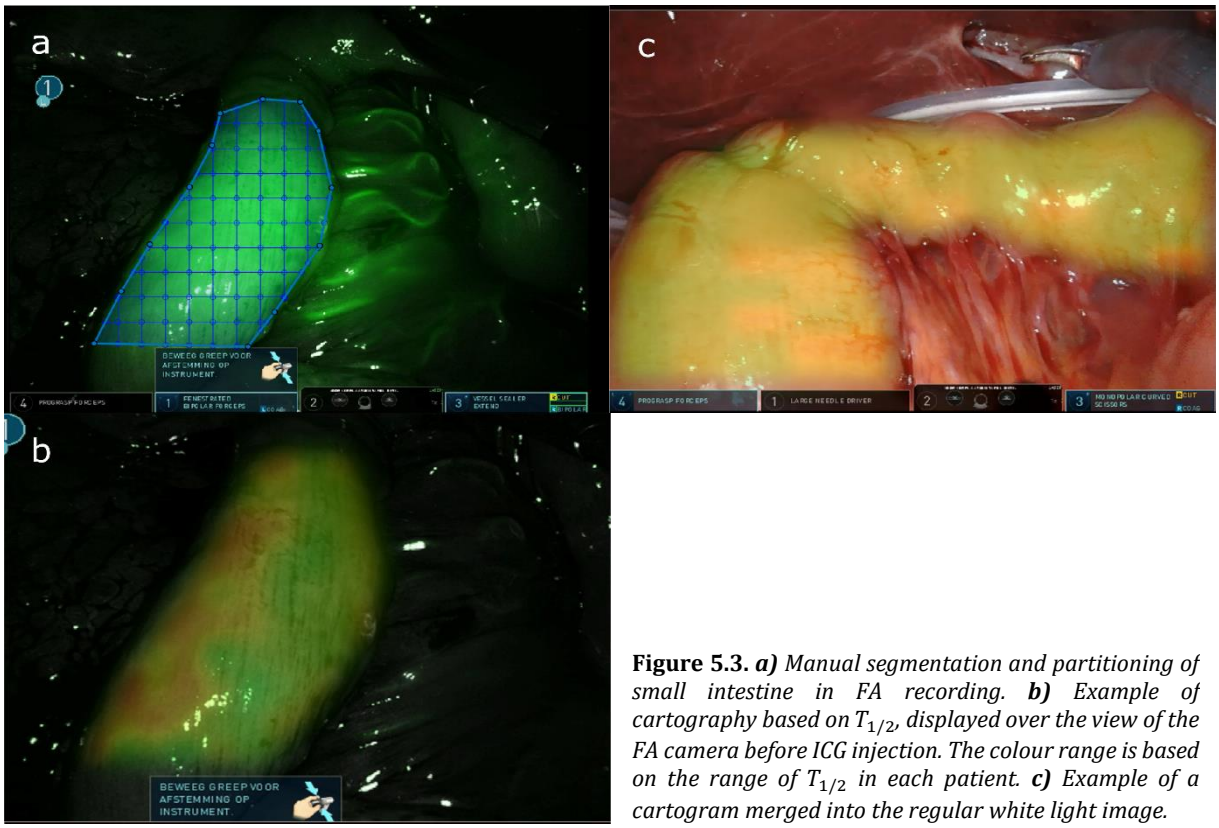

Figure 5.3. ***a)*** *Manual segmentation and partitioning of small intestine in FA recording.* ***b)*** *Example of cartography based on $T_{1/2}$, displayed over the view of the FA camera before ICG injection. The colour range is based on the range of $T_{1/2}$ in each patient.* ***c)*** *Example of a cartogram merged into the regular white light image.*

5.3.2 Patient analysis

A total of 32 patients were analysed using the developed algorithm. In Figure 5.2 boxplots are displayed that indicate the characteristics of $T_{1/2}$ in the small intestine for all included patients. The median value of $T_{1/2}$ varied between 2.1 and 9.1 seconds and the IQR varied between 0.3 and 2.9 seconds. Overall, $T_{1/2}$ had a median value of 5.1 (IQR = 2.4) seconds and a minimal and maximal value of 1.3 and 9.9 seconds respectively. The mean $T_{1/2}$ was found to be 5.2 (σ = 1.9) seconds, with 95% CI: 1.5 – 9.0.

Figure 5.3 shows two examples of a cartogram automatically generated based on the value of $T_{1/2}$, as well as the grid-based division of an intestinal segmentation.

5.4 Discussion

This pilot study demonstrated that an automated approach in the quantification of FA for peroperative intestinal perfusion assessment including the characteristics of FA parameter $T_{1/2}$ is feasible.

The ability of the changepoint detection algorithm was examined. Since there is no common consensus on the exact definition of T_0 and T_{max}, an inquiry on the input of nine independent human observers was performed. With intra-observer ICC's varying between 0.93 and 1.000, it was found that these observers allocated T_0 and T_{max} with excellent consistency. Moreover, the inter-observer ICC of 0.95 showed a great agreement between observers. This substantiated the decision to consider the input of multiple human observers as 'golden standard' in the evaluation of algorithm performance. The time-efficient changepoint detection algorithm showed excellent agreement with the observers (ICC = 0.95). This was considered as proper validation, advocating the use of an unsupervised method (applying the grid) in the analysis of $T_{1/2}$. The benefits of the

semi-automated algorithm are best illustrated with the presented cartograms. Immediate perfusion quantification can be achieved in large sections of the intestine with one injection of ICG.

Automated analysis of $T_{1/2}$ was performed in FA recordings of 32 normally perfused small intestines. The found mean value of 5,2 (σ = 1.9) seconds is considered to be fast, compared with results reported by Wada et al. and Son et al.[7,19] In these studies, colonic perfusion in patients who underwent surgery for colorectal cancer was quantitatively analysed using FA. Their presented mean values of $T_{1/2}$ were respectively 12,5 (σ = 7.6) and 11.7 (σ = 0.8) seconds for patients who did not develop AL. Based on the results of this pilot study, it is expected that $T_{1/2}$ values are generally lower in the small intestine compared with the large intestine. Son et al. showed a significant increase of $T_{1/2}$ in patients who presented AL, reporting a mean of 40.37 (σ = 7.8) seconds. Despite the number of patients with AL ($n = 6$) being relatively small, these results are promising for the establishment of a useful threshold value. The current study reveals a spread of parameter $T_{1/2}$ between 1.5 and 9.0 seconds in normally perfused small intestine. When in future research patients with impaired intestinal perfusion show values relatable to the AL cases presented by Son et al., a great predictive value could be achieved.

It should be considered that the single parameter $T_{1/2}$ is unlikely to portray the complete perfusion situation in a tissue area. Several circumstances can be imagined where impaired perfusion is not indicated by $T_{1/2}$. As described by Barberio et al., bowel tissue with extreme perfusion impairment might show a 'normal' value of a time-based parameter such as $T_{1/2}$.[21] When the intensity levels substantially decrease, a time to intensity threshold becomes severely inaccurate because the signal to noise ratio decreases. In this case a lot of information about the signal increase is lost, weakening the capability of time-based parameters. However, in the described situation of severely impaired transmural perfusion, the regular clinical judgement improves its informative value: black discoloured bowel tissue is not suitable for anastomosis, and it is insensible to perform FA in this situation. The value of quantified FA lies in marginal perfusion.[21] It is, however, unclear where the strength of clinical judgement stops and the benefit of FA begins.

In order to clarify the correct interpretation of quantified FA and be able to identify inadequate perfusion, the current study has to be expanded with more data. The presented approach is a substantial step towards an objective standardised method of analysis. When this is established, large scale data acquisition should be relatively straightforward. Naturally, the succeeding step would be to include patients with a known form of perfusion impairment. For instance, patients suffering from acute mesenteric ischemia (AMI) or chronic mesenteric ischemia (CMI) are certainly relevant. Indeed, one of the most important applications of FA is in the advanced stages of AMI or CMI.[22,23] In case of transmural ischemia, bowel tissue is often surgically removed. It is very likely that surrounding non-necrotic tissue is not properly perfused in this situation, increasing the risk of AL. A predictive threshold value in combination with the presented cartograms could be of great assistance in these circumstances.

A limitation in the current method is the lack of standardized admission of ICG. The rate and anatomical site at which the agent is injected influence the dilution in blood. This consequently affects intensity levels and fluorescence dynamics. It is therefore advised to investigate the use of an automated contrast injection system. Another presumably influential factor in the dynamics of

ICG is cardiac output. In case of high cardiac output, it can be expected that time-based perfusion parameters improve. Future work should investigate the effect of cardiac output on quantified FA parameters and consider a possible correction. Finally, it is advised to examine the effects of temperature on FA parameters. Due to consistent CO_2 insufflation, the temperatures during laparoscopy are expected to be similar. However, these conditions change when FA is applied in open procedures.

5.5 Conclusion

In conclusion, the presented semi-automated approach allows convenient analysis of FA recordings and can be of great assistance in the pursuit of threshold values to distinguish peroperative sufficient and impaired bowel wall perfusion. Clinical validation studies should be undertaken to underline that semi-automated FA analysis could reliably identify non-viable bowel tissue in gastrointestinal surgery.

Authors' Contributions

H.G.M.V., B.W., R.H.G., and D.J.L. designed the study. D.J.L. acquired data. H.G.M.V., B.W., R.H.G., and D.J.L. analyzed the data. All authors participated in data interpretation and article preparation.

Disclosure Statement

No competing financial interests exist.

Funding Information

No funding was received.

References

1. Platell C, Barwood N, Dorfmann G, Makin G. The incidence of anastomotic leaks in patients undergoing colorectal surgery. *Color Dis*. 2007;9(1):71-79.
2. Kingham TP, Pachter HL. Colonic Anastomotic Leak: Risk Factors, Diagnosis, and Treatment. *J Am Coll Surg*. 2009;208(2):269-278.
3. Turrentine FE, Denlinger CE, Simpson VB, et al. Morbidity, mortality, cost, and survival estimates of gastrointestinal anastomotic leaks. *J Am Coll Surg*. 2015;220(2):195-206.
4. Urbanavičius L. How to assess intestinal viability during surgery: A review of techniques. *World J Gastrointest Surg*. 2011;3(5):59.
5. Karliczek A, Harlaar NJ, Zeebregts CJ, Wiggers T, Baas PC, van Dam GM. Surgeons lack predictive accuracy for anastomotic leakage in gastrointestinal surgery. *Int J Colorectal Dis*. 2009;24(5):569-576.
6. Kawada K, Hasegawa S, Wada T, et al. Evaluation of intestinal perfusion by ICG fluorescence imaging in laparoscopic colorectal surgery with DST anastomosis. *Surg Endosc*. 2017;31(3):1061-1069.
7. Wada T, Kawada K, Takahashi R, et al. ICG fluorescence imaging for quantitative evaluation of colonic perfusion in laparoscopic colorectal surgery. *Surg Endosc*. 2017;31(10):4184-4193.
8. Kim JC, Lee JL, Park SH. Interpretative Guidelines and Possible Indications for Indocyanine Green Fluorescence Imaging in Robot-Assisted Sphincter-Saving Operations. *Dis Colon Rectum*. 2017;60(4):376-384.
9. Rønn JH, Nerup N, Strandby RB, et al. Laser speckle contrast imaging and quantitative fluorescence angiography for perfusion assessment. *Langenbeck's Arch Surg*. 2019;404(4):505-515.
10. Björck M, Koelemay M, Acosta S, et al. Editor's Choice e Management of the Diseases of Mesenteric Arteries and

Veins Clinical Practice Guidelines of the European Society of Vascular Surgery (ESVS). Published online 2017: DOI: 10.1016/j.ejvs.2017.01.010

11. Su H, Wu H, Bao M, et al. Indocyanine green fluorescence imaging to assess bowel perfusion during totally laparoscopic surgery for colon cancer. *BMC Surg*. 2020;20(1):1-7.

12. De Nardi P, Elmore U, Maggi G, et al. Intraoperative angiography with indocyanine green to assess anastomosis perfusion in patients undergoing laparoscopic colorectal resection: results of a multicenter randomized controlled trial. *Surg Endosc*. 2020;34(1):53-60.

13. Jafari MD, Wexner SD, Martz JE, et al. Perfusion assessment in laparoscopic left-sided/anterior resection (PILLAR II): A multi-institutional study. *J Am Coll Surg*. 2015;220(1):82-92.e1.

14. Diana M, Noll E, Diemunsch P, et al. Enhanced-reality video fluorescence: A real-time assessment of intestinal viability. *Ann Surg*. 2014;259(4):700-707.

15. Matsui A, Winer JH, Laurence RG, Frangioni J V. Predicting the survival of experimental ischaemic small bowel using intraoperative near-infrared fluorescence angiography. *Br J Surg*. 2011;98(12):1725-1734.

16. Lütken CD, Achiam MP, Svendsen MB, Boni L, Nerup N. Optimizing quantitative fluorescence angiography for visceral perfusion assessment. *Surg Endosc*. 2020;34(12):5223-5233.

17. Degett TH, Andersen HS, Gögenur I. Indocyanine green fluorescence angiography for intraoperative assessment of gastrointestinal anastomotic perfusion: a systematic review of clinical trials. *Langenbeck's Arch Surg*. 2016;401(6):767-775.

18. Nerup N, Andersen HS, Ambrus R, et al. Quantification of fluorescence angiography in a porcine model. *Langenbeck's Arch Surg*. 2017;402(4):655-662.

19. Son GM, Kwon MS, Kim Y, Kim J, Kim SH, Lee JW. Quantitative analysis of colon perfusion pattern using indocyanine green (ICG) angiography in laparoscopic colorectal surgery. *Surg Endosc*. 2019;33(5):1640-1649.

20. Vallance A, Wexner S, Berho M, et al. A collaborative review of the current concepts and challenges of anastomotic leaks in colorectal surgery. *Color Dis*. 2017;19(1):O1-O12.

21. Barberio M, Felli E, Seyller E, et al. Quantitative fluorescence angiography versus hyperspectral imaging to assess bowel ischemia: A comparative study in enhanced reality. *Surg (United States)*. Published online 2020: DOI: 10.1016/j.surg.2020.02.008

22. Karampinis I, Keese M, Jakob J, et al. Indocyanine Green Tissue Angiography Can Reduce Extended Bowel Resections in Acute Mesenteric Ischemia. *J Gastrointest Surg*. 2018;22(12):2117-2124.

23. Nakagawa Y, Kobayashi K, Kuwabara S, Shibuya H, Nishimaki T. Use of indocyanine green fluorescence imaging to determine the area of bowel resection in non-occlusive mesenteric ischemia: A case report. *Int J Surg Case Rep*. 2018;51:352-357.

6 Intra-operative Quantification of Fluorescence Angiography for Assessment of Intestinal Perfusion: An In Vivo Exploration of Clinical Value

H.G.M. Vaassen BSc,[a] B. Wermelink MSc,[a, b] S. Manohar, Prof., PhD, R.H. Geelkerken, Prof., MD, PhD,[a, b] and D.J. Lips, MD, PhD[c]

[a] Multi-Modality Medical Imaging (M3i) group, TechMed Centre, University of Twente, Enschede, The Netherlands
[b] Section Vascular Surgery and [c] section Gastrointestinal and Oncology Surgery, Department of Surgery, Medisch Spectrum Twente, Enschede, The Netherlands

Manuscript submitted and under review – December 2021

Abstract

Background – Fluorescence angiography (FA) could provide the highly required quantification of intestinal perfusion. In this observational pilot study, we aimed to develop a reliable and easily implementable FA quantification method, and investigated the correlation of inflow parameters with in vivo intestinal perfusion status.

Materials and Methods – Algorithms for the on-site extraction of FA inflow parameters time to peak (TTP) and normalized peak slope (NPS) were developed. A database of 32 FA recordings in patients without impaired bowel perfusion was analysed to provide a reference frame of healthy values. Nine patients with suspected bowel perfusion impairment, of which seven underwent a restoration of vascularization, were prospectively included.

Results – Patients without impaired intestinal perfusion displayed a median TTP of 4.8 (IQR = 2.5) seconds and a median NPS of 12.8 (IQR = 5.1) %/second, with 95% of the measurements resulting in TTP under 7.0 seconds and NPS over 9.4 %/second. The group with suspected impaired perfusion showed a significantly different median TTP of 9.6 (IQR = 3.2, $P < 0.01$) seconds and median NPS of 7.3 (IQR = 1.9, $P < 0.01$) %/second. Seven of these patients (78%) exhibited inflow parameters outside the healthy range before revascularization. FA quantification displayed a clear recovery of inflow in six of seven patients where vascularization was restored.

Conclusions – The presented on-site FA quantification is directly implementable and correlates with intestinal perfusion status and corresponding symptoms, showing great potential for detecting perfusion impairment. Future research should define FA parameter ranges for various perfusion requirements, predicting clinical outcomes.

*This chapter contains the manuscript that represents the first results of the single-centre FLIGHT study. The acronym FLIGHT is derived from '**FL**uorescence **I**maging for **G**astrointestinal **H**emodynamics **T**rial'. It identifies the ongoing observational study regarding FA and intestinal perfusion, but also stands for the dedicated research group in MST that pursues the clinical implementation of quantified FA.*

6.1 Introduction

Despite great technological advancements in gastro-intestinal surgery, incidences of anastomotic leakages (AL) are still reported between 3% and 19%.[1] Perfusion status of the anastomosis site is regarded as one of the most critical factors in the aetiology of AL.[2] In current practice, this is commonly evaluated by means of clinical observations such as serosa discoloration, palpable pulsations and bleeding from the marginal artery. However, this method is subjective and it has previously been shown that surgeons lack predictive accuracy regarding AL.[3] Likewise, the decision to resect suspected inviable tissue in case of acute mesenteric ischemia (AMI) or bowel incarceration, where perfusion status is key, is also most often based on clinical inspection and surgeon's experience. This is undesirable, bearing in mind the crucial consideration between the risk of residual necrosis and peritonitis on one hand, and the risk of short bowel syndrome on the other.[4,5] Consequently, there is a need for objective and reliable intraoperative assessment of intestinal perfusion.

Fluorescence angiography (FA), which entails intravenously injecting contrast agent indocyanine green (ICG) and monitoring its appearance in tissue using near-infrared (NIR) light, has emerged as an intraoperative tool with great potential in perfusion assessment. Its superiority over subjective clinical judgement in the evaluation of blood supply has been shown in experimental models, but randomized controlled trials did not show a significant reduction in AL.[6–9] The main reason for this is the qualitative interpretation of FA images, resulting in low repeatability and high inter-observer variability.[10] Multiple reviews have therefore deduced that FA quantification based on intensity-over-time curves is the way forward.[11–13] However, quantitative assessment of the acquired data is a great challenge due to the lack of standardization in measurement protocols, absence of robust metrics for ICG kinetics, and paucity of reference quantified data in healthy and impaired perfusion situations.[14,15]

A review by Lütken et al. exhibited the predictive potential of previously investigated parameters, but at the same time illustrated the great inconsistency between different studies with regard to threshold values.[14] This is largely attributable to the use of intensity-based parameters, which are very sensitive to variations in measurement circumstances. Influential factors like distance to light source, camera angulation, light absorption/scattering and ICG distribution in plasma are extremely difficult to reproduce in an operative setting. This severely decreases the measurement precision and prohibits the universal use of threshold values. From a theoretical point of view, inflow-based parameters that display the speed, rather than the total amount of ICG arrival, circumvent these influences and should therefore be more robust. Various clinical studies showed that inflow-based parameters have strong predictive value regarding AL, while also presenting consistent values in the 'non-AL' groups. For example, studies by Son et al. and Wada et al. reported similar times to reach half of maximal intensity at respectively 11.7 (± 0.8) and 12.5 (± 7.6) seconds, while the mean maximal intensity was reported at distinct values of 58.0 (± 3.4) and 91.4 (± 31.9), respectively.[16,17]

In addition to bearing predictive value, FA parameters must allow automatic and reliable extraction to be instantaneously applicable in an intraoperative decision-making system. Many of the previously investigated inflow-based parameters rely on the identification of the start-and endpoint of the intensity increase (T_0 and T_{max}), which are often ambiguous and hard to point out objectively.[14,18,19]

In this study, we present a method that allows semi-automatic on-site quantification of bowel perfusion based on inflow parameters and does not involve T_0 and T_{max}. Furthermore, we demonstrate the clinical potential by presenting nine cases involving impaired mesenteric circulation alongside a collection of measurements in patients with uncompromised intestinal perfusion.

6.2 Materials & Methods

6.2.1 Patient inclusion

A total of nine patients were prospectively included in this single-centre observational study, according to the following inclusion criteria: radiologically (CT-angiography) or surgically confirmed mesenteric ischemia or small bowel incarceration, requiring laparoscopic or open surgery according to current best clinical practice, and a minimum age of 18 years. The local medical-ethical review committee granted approval for the study and written informed consent for publication of the data was received from all included patients. Characteristics of these patients, diagnosis and performed intervention are presented in Table 6.1. Patients were divided into three groups, according to the performed surgery. Patients in group A were diagnosed with chronic mesenteric ischemia (CMI) and were treated with an operative superior mesenteric artery (SMA) revascularization. Group B consisted of patients who were diagnosed with AMI and underwent emergency laparotomy. Patients in group C underwent emergency laparoscopy where an incarcerated small bowel obstruction was observed. In order to provide a reference frame for the comparison with normal FA parameters, our prospectively collected database, composed of 32 FA recordings in patients undergoing bowel-unrelated surgery, was retrospectively analysed.[18]

6.2.2 Surgical procedure and data acquisition

FA was performed by intravenous injection of 5mg ICG (5mg/ml, Verdye, Diagnostic Green GmbH, Aschheim-Dornach, Germany) and subsequent saline flushing. NIR-imaging data was obtained using the monochromatic NIR mode of the laparoscopic IMAGE1 S™ RUBINA system (Karl Storz, GmbH and Co., KG, Tüttlingen, Germany). Parallel to the regular imaging chain, live video frames were transmitted to a personal computer through an HDMI frame grabber for real-time analysis. No clinical decisions were made based on the FA quantification analysis.

During open surgical procedures, the lighting in the operation room was dimmed and the laparoscopic camera optic was held over the bowel while fixated to the operation table. In the cases of group A, measurements were conducted on a jejunum segment approximately 50 cm distal of Treitz's ligament and on an ileum segment approximately 30 cm proximal of the coecum. A small suture mark was placed on the visceral mesentery to enable consistent measurements before and after the procedure. The segment that appeared most compromised on FA prior to revascularization was selected for analysis in this study. In groups B and C, measurements were performed on an affected bowel segment as identified on visual inspection. In the event that ICG inflow was completely absent, rendering analysis of inflow dynamics unfeasible, the closest neighbouring tissue that displayed inflow was selected for quantification analysis. Since the patients in group C suffered from a strangulated bowel segment, there was no reason to suspect impaired perfusion elsewhere. This allowed for a reference measurement in an unaffected

Table 6.1. Baseline characteristics and specifics on diagnosis and performed intervention of patients with suspected bowel perfusion impairment (n = 9).

Group	Pt. #	Sex	Age	BMI	ASA	Vascular risk factors	Diagnosis	Intervention
A	1	F	78	24.2	IV	-	2-Vessel (CA/SMA) CMI	CIA to SMA graft*
	2	F	53	35.9	II	HT, HL	2-Vessel (CA/SMA) CMI	EIA to SMA graft#
	3	M	66	29.3	IV	DM2, HT, HL, PAD, Smoking	3-Vessel AoCMI	Antegrade aortic to SMA graft*
	4	M	56	24.8	III	-	1-Vessel (SMA) AoCMI	Patch angioplasty SMA#
	5	F	38	22.7	III	PAD, Smoking	3-Vessel CMI	Aortic endarterectomy, retrograde aortic to SMA and CHA graft#
B	1	M	57	Unknown	V	DVT, PAD	3-Vessel AMI	Laparotomy – no further actions
	2	M	65	21.2	IV	CVA, HT, PAD	2-Vessel AoCMI	Ileum/coecum resection
C	1	M	63	24.1	I	Smoking	Herniation-induced SBS	Laparoscopic release
	2	M	61	27.2	II	AF, HT, HL, Smoking	Adhesion-induced SBS	Laparoscopic release

AF, atrial fibrillation; *AMI,* acute mesenteric ischemia; *AoCMI,* acute-on-chronic mesenteric ischemia; *ASA,* American Society of Anaesthesiologists; *BMI,* body-mass index; *CA,* coeliac artery; *CHA,* common hepatic artery; *CIA,* common iliac artery; *CMI,* chronic mesenteric ischemia; *CVA,* cerebro vascular accident; *DM2,* type 2 diabetes mellitus; *DVT,* deep vein thrombosis; *EIA,* external iliac artery; *HL,* hyperlipidaemia; *HT,* hypertension; *PAD,* peripheral artery disease; *SBS,* small bowel strangulation; *SMA,* superior mesenteric artery; * Prosthetic; # Autogenous

segment. The bowel segments that were included for analysis were clinically scored on vitality according to a three-point Likert scale, which is illustrated in the Supplementary Table (Appendix D).

6.2.3 Quantification and analysis

FA data was analysed using an in-house developed software tool, written in Python (Python Software Foundation, Wilmington, DE, USA). RGB frames were captured at 10 frames/second and converted to a luminance map. Intensity-over-time curves were generated by monitoring the luminance value of a specific pixel or region of interest (ROI) along the data frames. Two parameters were defined for analysis: time to peak (TTP) and normalized peak slope (NPS). TTP was defined as the time between reaching $I_{20\%}$ and $I_{80\%}$, which are calculated according to:

$$I_{20\%} = I_{0\%} + 0.2 \times (I_{100\%} - I_{0\%}) \quad (6.1)$$

$$I_{80\%} = I_{0\%} + 0.8 \times (I_{100\%} - I_{0\%}) \quad (6.2)$$

$I_{0\%}$ and $I_{100\%}$ are the baseline and maximum intensity, which are calculated by taking the median value of respectively the ten lowest and ten highest data samples of the curve.

For determining NPS, the signal is convolved with a finite impulse response differentiation filter with a window size of 75 data points. This operation filters the signal and computes the first derivative. Peak slope (PS) is the maximum value of the output, and is considered as the maximal slope in the signal that is not originating from high frequent noise or artefacts such as peristalsis.

For the purpose of being solely inflow-based, PS is normalized and converted to units [%/second] by:

$$NPS = \frac{PS}{I_{100\%} - I_{0\%}} \times 10 \times 100\% \tag{6.3}$$

After ICG inflow has occurred, the software allows the user to interactively draw and move ROI's over either the FA recording or the live video footage for direct signal quantification and analysis. Moreover, both parameters could be calculated for all pixels individually and displayed as a heatmap within 5-10 seconds, enabling direct integration of the quantification in the live (white light) footage.

Distributions of TTP and NPS were described using the median and interquartile range (IQR). Significant differences between groups were evaluated using Mood's median test, with *P*-value < 0.05 considered as significant. Values of TTP were considered within the healthy range when they were lower than the 95th percentile of the group without perfusion impairment, while NPS values were considered healthy when exceeding the 5th percentile.

6.3 Results

Retrospective analysis of our database containing FA recordings of unimpaired bowel perfusion provided a median TTP of 4.8 (IQR = 2.5) seconds, with 95% of measurements under 7.0 seconds. Median NPS was found to be 12.8 (IQR = 5.1) %/second, with 95% of measurements over 9.4 %/second.

Results of the quantified FA analysis in patients with suspected bowel perfusion impairment are displayed in Table 6.2. This group showed a median TTP of 9.6 (IQR = 3.2) seconds and median NPS of 7.3 (IQR = 1.9) %/second, both significantly different compared with the unimpaired group ($P < 0.01$). Measurements after the vascularization was restored provided a median TTP of 4.2 (IQR = 1.6) seconds and a median NPS of 14.5 (IQR = 3.3) %/second, which differed significantly from the medians before intervention ($P = 0.03$). In Figure 6.1, the measurements before and after revascularization are presented next to a violin plot depicting the distributions of TTP and NPS in the uncompromised bowel perfusion group. Seven out of nine patients (78%) with suspected bowel perfusion impairment displayed inflow parameters outside the healthy range. Moreover,

Table 6.2. Results of quantified FA analysis in patients with impaired mesenteric circulation.

Group	Pt. #	TTP (seconds)			NPS (%/second)			Clinical judgement*
		Pre	Post	Reference	Pre	Post	Reference	
A	1	8.7	4.7	-	7.8	15.0	-	VI – PI
	2	5.8	6.4	-	10.8	11.7	-	VI – PI
	3	10.2	3.9	-	6.6	18.5	-	VI – PI
	4	18.6	4.2	-	6.2	14.5	-	VI – PI
	5	10.9	8.5	-	6.1	8.6	-	VI – PI
B	1	8.9	-	-	7.5	-	-	VI – PII
	2	8.2	-	-	8.6	-	-	VII – PI
C	1	11.8	4.1	3.7	7.1	14.2	15.2	VIII
	2	6.9	3.9	4.3	9.1	17.5	15.5	VII

***** Scored before revascularization based on visual inspection (V) and palpation (P) as either I (most likely reversible or no transmural ischemia), II (dubious reversibility of ischemia) or III (most likely irreversible, transmural ischemia/necrosis)

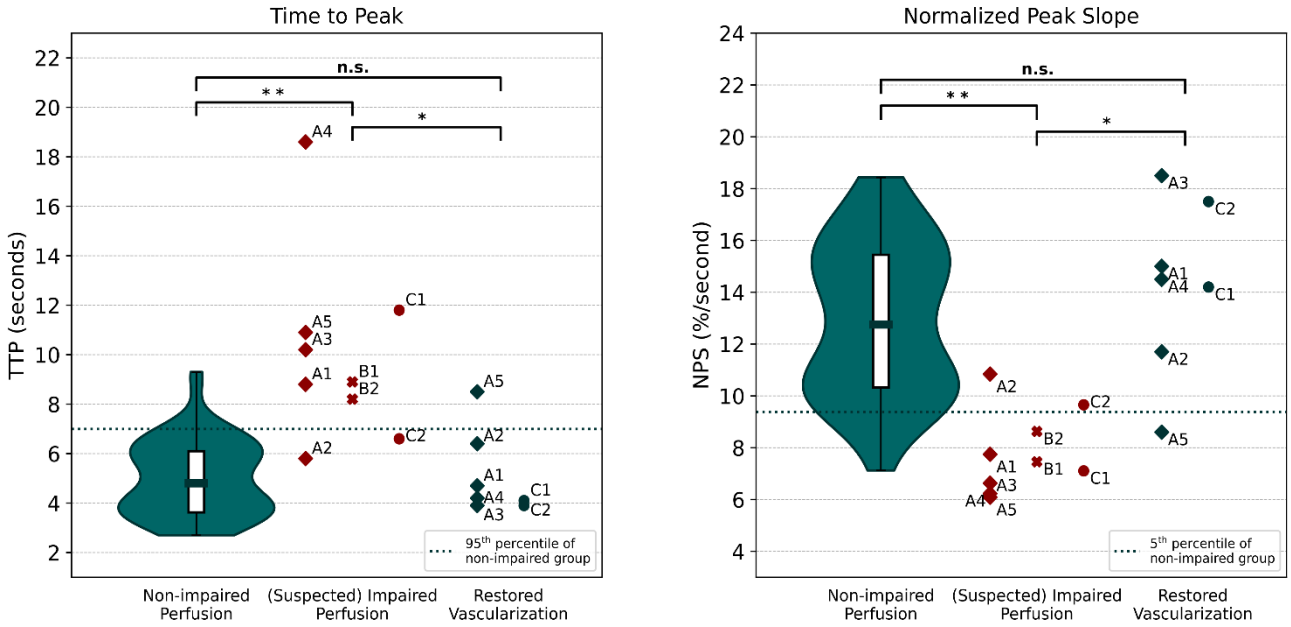

Figure 6.1. *Violin plots showing the distribution of FA parameters in the group with no perfusion impairment, along with scatter plots presenting the measured parameters in patients with (suspected) bowel perfusion impairment before and after revascularization. Mood's median test: **P<0.01, *P<0.05,* ***n.s.*** *non-significant.*

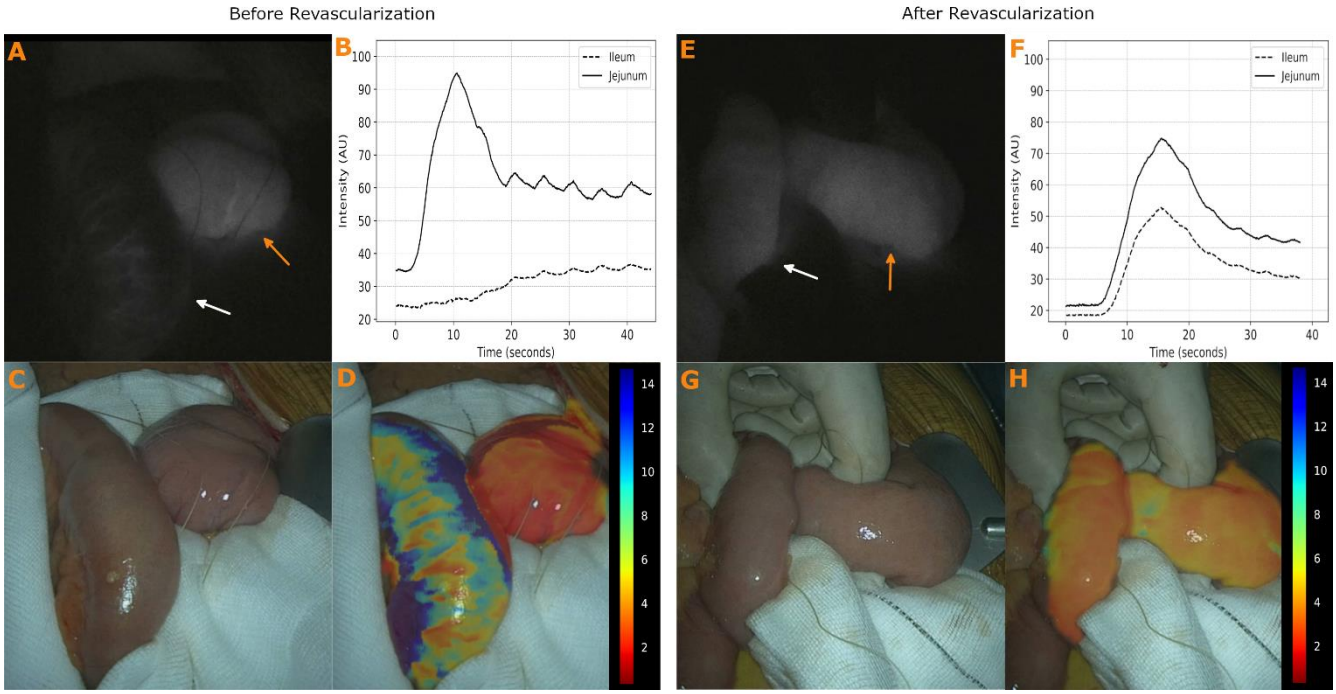

Figure 6.2. *Intraoperative FA analysis of patient A4 before (**left** panel) and after (**right** panel) SMA revascularization. White arrow indicates ileum, orange arrow indicates jejunum.* ***(A/E)*** *Monochromatic NIR mode.* ***(B/F)*** *Intensity-over-time curves of the jejunal and ileal segment.* ***(C/G)*** *White light imaging mode.* ***(D/H)*** *Heatmap based on TTP overlayed on white light footage.*

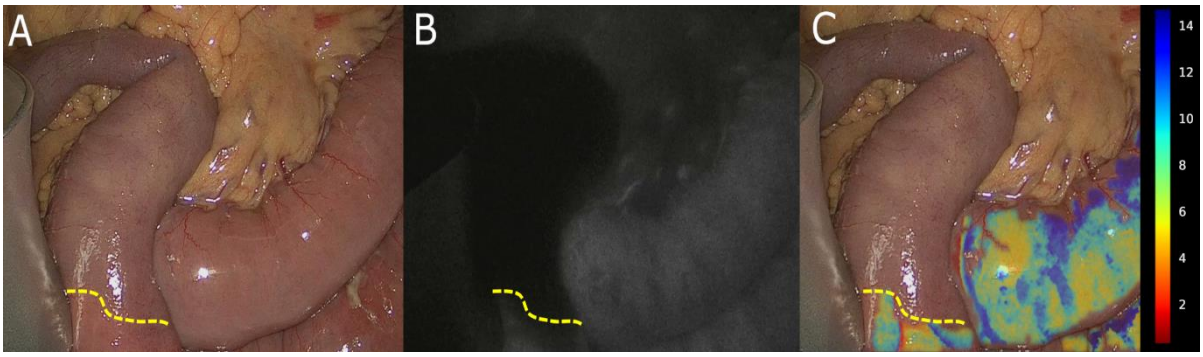

Figure 6.3. *Intraoperative footage of patient B2 in **(A)** white-light mode, **(B)** NIR mode and **(C)** with TTP heatmap. The dotted line represents the border of the segment with purple discoloration that was detected by FA as non-perfused.*

six of the seven patients in groups A and C showed evident improvement of inflow parameters after vascularization was restored. Five of these patients showed recovery into the normal range, all of whom had excellent clinical outcome. Figure 6.2 depicts the FA analysis and visual inspection before and after SMA revascularization in patient A4, illustrating such a recovery. Note the similar appearance on visual inspection (Fig. 6.2C/6.2G), but considerable differences on qualitative (Fig. 6.2A/6.2E) and quantitative (Fig. 6.2D/6.2H) FA.

None of the CMI patients in group A exhibited visual or palpable signs of intestinal ischemia during surgery. Patients A1, A3 and A4 were completely relieved of CMI symptoms and could be discharged with a normal diet. Patient A2 had a history of recanalization and stenting procedures in the coeliac artery (CA) and SMA. She presented with atypical abdominal complaints and an in-stent SMA stenosis. Although her symptoms were not typical for CMI, she was selected for a bypass based on previous clinical improvements after endovascular treatment. Nevertheless, her complaints recurred within several weeks postoperatively, in spite of CT angiography showing a patent bypass with proper filling of distal SMA branches. Patient A5 received bypass grafts on the SMA and common hepatic artery as well as aortabi-iliac endarterectomy as treatment for three-vessel CMI, but showed negligible improvement of inflow parameters in the ileum. The SMA bypass was found to be occluded one day after surgery. Re-laparotomy was performed and thrombectomy of the bypass resulted in a slight increase in inflow dynamics, with parameters still outside the 95th percentile of the normal perfusion group. Unfortunately, the patient did not survive the postoperative course due to major complications including bypass re-occlusion, AMI, bleeding, abdominal compartment syndrome and multiple organ failure.

Patient B1 underwent laparotomy for AMI, where a gangrenous intestinal tract distal of the duodenum was observed. FA displayed a complete lack of ICG inflow in these segments. Moreover, FA identified several patches of duodenum as non-perfused, while they still appeared viable on visual inspection. Tissue that did show ICG inflow resulted in parameters outside the healthy range. Due to the extent of necrosis, the procedure was aborted without revascularization or resection and the patient died afterwards. Laparotomy in patient B2 revealed a necrotic coecum and a slight cyanotic discoloration of an ileum segment. FA revealed complete lack of ICG inflow in these segments (see Fig. 6.3). Neighbouring ileum appeared vital, but resulted in inflow parameters outside the healthy range. Based on the absence of doppler signals, 20 cm of ileum was resected along with the coecum, after which the patient was relieved of symptoms.

In group C, both patients were successfully treated with a laparoscopic release of the small bowel strangulation. The strangulated segment of patient C1 was deemed as irreversibly ischemic by an experienced gastroenterological surgeon, but the initial decision to perform resection was overturned when arterial inflow was observed on qualitative FA. After release of the strangulation, this arterial inflow increased considerably. In agreement with these findings, quantitative FA analysis revealed a clear recovery from abnormal to healthy inflow parameter values. In patient C2, red discoloration of the strangulated bowel was observed, possibly indicating ischemia. FA quantification before release did not result in values outside the healthy range, but release of the strangulation did result in a clear improvement.

6.4 Discussion

Peroperative evaluation of intestinal perfusion is critical in various surgical affairs, but it is generally performed based on subjective and fallible clinical observations. In addition, the limited haptic evaluation of tissue has withheld minimally invasive surgery from being applied in cases of compromised bowel perfusion.[20,21] Previous work showed that quantified FA has the potential to provide objective and accurate perfusion assessment peroperatively. The aim of this pilot study was to implement a real-time FA analysis method that can be integrated in the workflow in the operating theatre immediately, and to investigate its potential for detecting impaired intestinal perfusion. Behaviour of FA parameters was investigated by conducting the analysis on FA imaging of patients without suspected bowel perfusion impairment and on patients with a known form of compromised bowel perfusion.

Quantitative FA analyses in the unimpaired bowel perfusion group produced a reference frame, with 95% of cases showing TTP under 7.0 second and NPS over 9.4 %/second (see Fig. 6.1). The majority (78%) of the compromised bowel perfusion group displayed inflow parameters outside this range before intervention, and revascularization resulted in a clear improvement on quantified FA in all but one patient, who died of multiple organ failure. This indicates that inflow-based FA quantification is accurate to predict changes in mesenteric perfusion status. Moreover, none of the five patients in group A exhibited visual signs of intestinal ischemia during surgery, while FA inflow parameters detected impaired perfusion in four of these cases. The corresponding perfusion states had not led to transmural ischemia, but clinical symptoms indicated compromised bowel function resulting from mucosal ischemia. It can be expected that the equivalent oxygen supply would be insufficient for wound healing, i.e. the healing of anastomoses. Additionally, in the case of patient A5, it can be argued that the lack of improvement in ICG inflow in the ileum indicated a malfunctioning SMA bypass graft. These findings show that the FA quantification method is able to provide critical additional information.

The results in patients A2 and C2 can be regarded as unexpected. Patient A2 displayed inflow parameters within the established healthy range and no increased inflow after intervention (see Fig. 1). However, the atypical nature of her symptoms, together with recurrence in spite of a patent bypass graft, could suggest that they had no clear relation with compromised intestinal perfusion. Patient C2 also displayed parameters within the healthy range prior to intervention, even though visual signs indicated compromised perfusion. Considering the fact that the inflow improved to values similar to healthy neighbouring tissue after intervention, it is presumed that the measured parameters represented impaired perfusion in this patient. The decreased inflow might, however,

not have been critical. Perfusion impairment in bowel strangulation is most often caused by venous occlusion, resulting in locally increased hemodynamic pressures. Consequential symptoms, such as haemorrhagic discoloration and oedema, may be misinterpreted as advanced ischemia.[22] Indeed, quantified FA could aid in differentiating between venous congestion and irreversible oxygen deficiency.

The influence of systemic hemodynamics and ICG distribution on perfusion measurements might also be explanatory for unexpected results. Using relative parameters, as suggested in literature, can be considered to address this issue.[7] Relative parameters are determined by comparing measurements with the signal that displays the best perfused segment, and thereby eliminating the effects of cardiac output, injection rate, dosage etc. However, the feasibility of this approach is debatable for a number of reasons. First, the absolute best perfused region is uncertain, since only a limited segment of bowel can be captured on FA. Second, the results in group A show that intestinal perfusion can be strongly impaired without any visual indication, meaning that a bowel segment might be falsely designated as healthy. Another promising method that considers hemodynamic state involves the correction of perfusion parameters with respect to contrast dynamics in supplying arteries. Elliot et al. performed elaborate simulations to illustrate the value of correcting the intensity-time curve using an arterial input function, as measured by a pulse-oximeter-style probe.[23] Future research must demonstrate the feasibility of this method in an in vivo setting.

Based on our results, the presented method of FA quantification has great potential for detecting intestinal perfusion impairment. Using inflow-based parameters ensures easy implementation in the clinical workflow, since most measurement circumstances do not need to be standardized. The strength of inflow-based parameters is illustrated in the example of patient A4 (see Fig. 6.2), where the inflow improves after revascularization while maximal intensity levels decrease (Fig. 6.2B/6.2F). The fast parameter extraction furthermore enables on-site analysis and direct integration by means of parametric mapping onto live footage (Fig. 6.2D/6.2H). Nevertheless, in order to transform quantified FA into a robust clinical decision-making system, several steps are still to be undertaken. First, although inflow-parameters eliminate many effects of measurement circumstances in theory, the current approach using RGB video-signals is not optimal. All analysis is based on the assumption that the irradiance of the camera sensor and the pixel intensity values are related in a consistent linear fashion, and that saturation of the light intensity, i.e. reaching maximum pixel value, is not the case. Quantification should ideally be based on the unprocessed irradiance data. Second, threshold values should be pursued for various surgical situations. Relieving mesenteric ischemia symptoms, preventing transmural ischemia and anastomotic healing are different processes and require different levels of perfusion. We envision a system that differentiates perfusion parameters into definitely sufficient, definitely insufficient and a range of dubious values where clinical factors such as extent of resection need to be considered. It should be noted that not all analysis can be inflow-based. In case of severe perfusion impairment, such as the two cases in group C, the FA signal will be insufficient for accurate analysis. A lack of perfusion is often straightforward to observe, but risk of misinterpretation due to misleading measurement circumstances remains present.[10] Some level of user experience is consequently still required.

This is the first study to illustrate the direct effects on quantified FA inflow parameters after mesenteric revascularization in an in vivo setting. Limitations in this study were the heterogeneity and relatively small size of the group with impaired bowel perfusion. Moreover, the analysis of the healthy perfusion group was retrospective and the designation of ROI's was performed manually, possibly inducing bias. Efforts to reduce this bias included ROI drawing without direct knowledge of quantification results and capturing as much bowel as possible in one ROI. Prior to implementation in clinical decision-making, the developed algorithms require external validation.

6.5 Conclusion

In this study, we presented a directly implementable on-site FA quantification method and demonstrated the correlation of FA parameters with intestinal perfusion status and corresponding symptoms, indicating great predictive potential for identifying impaired perfusion. Further sufficiently powered clinical trials should define FA thresholds for various perfusion requirements.

Disclosure Statement

No competing financial interests exist.

Funding Information

No funding was received.

References

1. Turrentine FE, Denlinger CE, Simpson VB, Garwood RA, Guerlain S, Agrawal A, et al. Morbidity, mortality, cost, and survival estimates of gastrointestinal anastomotic leaks. J Am Coll Surg. 2015;220(2):195–206.
2. Thompson SK, Chang EY, Jobe BA. Clinical review: Healing in gastrointestinal anastomoses, part I. Vol. 26, Microsurgery. 2006. p. 131–6.
3. Karliczek A, Harlaar NJ, Zeebregts CJ, Wiggers T, Baas PC, van Dam GM. Surgeons lack predictive accuracy for anastomotic leakage in gastrointestinal surgery. Int J Colorectal Dis. 2009;24(5):569–76.
4. Tilsed JVT, Casamassima A, Kurihara H, Mariani D, Martinez I, Pereira J, et al. ESTES guidelines: acute mesenteric ischaemia. Vol. 42, European Journal of Trauma and Emergency Surgery. 2016. p. 253–70.
5. Karampinis I, Keese M, Jakob J, Stasiunaitis V, Gerken A, Attenberger U, et al. Indocyanine Green Tissue Angiography Can Reduce Extended Bowel Resections in Acute Mesenteric Ischemia. J Gastrointest Surg. 2018 Dec 1;22(12):2117–24.
6. Matsui A, Winer JH, Laurence RG, Frangioni J V. Predicting the survival of experimental ischaemic small bowel using intraoperative near-infrared fluorescence angiography. Br J Surg. 2011;98(12):1725–34.
7. Diana M, Agnus V, Halvax P, Liu YY, Dallemagne B, Schlagowski AI, et al. Intraoperative fluorescence-based enhanced reality laparoscopic real-time imaging to assess bowel perfusion at the anastomotic site in an experimental model. Br J Surg. 2015;102(2):169–76.
8. De Nardi P, Elmore U, Maggi G, Maggiore R, Boni L, Cassinotti E, et al. Intraoperative angiography with indocyanine green to assess anastomosis perfusion in patients undergoing laparoscopic colorectal resection: results of a multicenter randomized controlled trial. Surg Endosc. 2020;34(1):53–60.
9. Jafari MD, Wexner SD, Martz JE, McLemore EC, Margolin DA, Sherwinter DA, et al. Perfusion assessment in laparoscopic left-sided/anterior resection (PILLAR II): A multi-institutional study. J Am Coll Surg. 2015;220(1):82-92.e1.
10. Dalli J, Hardy N, Mac Aonghusa PG, Epperlein JP, Cantillon Murphy P, Cahill RA. Challenges in the interpretation of colorectal indocyanine green fluorescence angiography – A video vignette. Vol. 23, Colorectal Disease. 2021.

p. 1289–90.

11. Degett TH, Andersen HS, Gögenur I. Indocyanine green fluorescence angiography for intraoperative assessment of gastrointestinal anastomotic perfusion: a systematic review of clinical trials. Langenbeck's Arch Surg. 2016;401(6):767–75.

12. Jansen SM, De Bruin DM, Van Berge Henegouwen MI, Strackee SD, Veelo DP, Van Leeuwen TG, et al. Optical techniques for perfusion monitoring of the gastric tube after esophagectomy: A review of technologies and thresholds. Vol. 31, Diseases of the Esophagus. 2018.

13. Slooter MD, Eshuis WJ, Cuesta MA, Gisbertz SS, van Berge Henegouwen MI. Fluorescent imaging using indocyanine green during esophagectomy to prevent surgical morbidity: A systematic review and meta-analysis. J Thorac Dis. 2019;11(1):S755–65.

14. Lütken CD, Achiam MP, Svendsen MB, Boni L, Nerup N. Optimizing quantitative fluorescence angiography for visceral perfusion assessment. Surg Endosc. 2020;34(12):5223–33.

15. Vallance A, Wexner S, Berho M, Cahill R, Coleman M, Haboubi N, et al. A collaborative review of the current concepts and challenges of anastomotic leaks in colorectal surgery. Color Dis. 2017;19(1):O1–12.

16. Son GM, Kwon MS, Kim Y, Kim J, Kim SH, Lee JW. Quantitative analysis of colon perfusion pattern using indocyanine green (ICG) angiography in laparoscopic colorectal surgery. Surg Endosc. 2019;33(5):1640–9.

17. Wada T, Kawada K, Takahashi R, Yoshitomi M, Hida K, Hasegawa S, et al. ICG fluorescence imaging for quantitative evaluation of colonic perfusion in laparoscopic colorectal surgery. Surg Endosc. 2017;31(10):4184–93.

18. Vaassen HGM, Wermelink B, Geelkerken RH, Lips DJ. Fluorescence-Based Quantification of Gastrointestinal Perfusion: A Step Towards an Automated Approach. J Laparoendosc Adv Surg Tech. 2021 Mar 19;

19. Meijer RPJ, van Manen L, Hartgrink HH, Burggraaf J, Gioux S, Vahrmeijer AL, et al. Quantitative dynamic near-infrared fluorescence imaging using indocyanine green for analysis of bowel perfusion after mesenteric resection. J Biomed Opt. 2021 Jun 9;26(06):060501.

20. Guerra F, Coletta D, Greco PA, Eugeni E, Patriti A. The use of indocyanine green fluorescence to define bowel microcirculation during laparoscopic surgery for acute small bowel obstruction. Color Dis. 2021;23(8):2189–94.

21. Johnson KN, Chapital AB, Harold KL, Merritt M V., Johnson DJ. Laparoscopic management of acute small bowel obstruction: Evaluating the need for resection. J Trauma Acute Care Surg. 2012;72(1):25–31.

22. Geelkerken RH, Cannegieter SC, Bouter H, van Bockel JH. Acute splanchnic venous thrombosis: surgical and medical treatment with special emphasis on new aspects of coagulation disorders. Eur J Vasc Endovasc Surg. 1997;13(2):227–32.

23. Elliott JT, Addante RR, Slobegean G-P, Jiang S, Henderson ER, Pogue BW, et al. Intraoperative fluorescence perfusion assessment should be corrected by a measured subject-specific arterial input function. J Biomed Opt. 2020;25(06):1.

7 General discussion

7.1 Summary

The work described in this thesis provided the first steps in transforming FA into a powerful intraoperative tool for the crucial assessment of local intestinal perfusion. Various algorithms were designed to quantify FA data based on inflow dynamics, and accompanying software was developed to allow application in the operating theatre. The first clinical demonstrations provided promising results.

Initial attempts for quantification were based on the detection of the start-and endpoint of intensity increase using an objective, automated approach. This showed promising results in a control group with normal intestinal perfusion, but signals of slow inflow impaired the performance. In addition, calculations required significant computational cost, making parametric mapping unfeasible. For this reason, new methods were adopted for the calculation of previously undefined parameters. These methods allowed the development of a software tool that provides live quantification.

The clinical potential of these parameters was established in a pilot study, where patients with a known form of compromised bowel perfusion were included. Not only was there a clear distinction between the quantification in these patients and the control group, but revascularization also resulted in a recovery of the parameters into the healthy range. The preliminary findings of the FLIGHT study show great potential for intraoperative detection of impaired perfusion. The study also revealed that quantified FA was able to detect areas of impaired perfusion that were not visible on clinical inspection. In most of these patients, the perfusion status would probably not have led to necrosis, but the mucosal function was impaired to such a degree that the patient experienced symptoms. It is unlikely that these bowel segments would provide adequate anastomotic healing, which would not have been suspected on clinical inspection. This illustrates the clinical need that is being addressed by quantified FA.

External validation showed that the current results need to be viewed with caution, and not be interpreted for general threshold values. Phantom experiments, described in Chapter 4, showed that NIR imaging systems are not optimized for quantification, but for qualitative observations and a ‘pleasant’ viewing experience. Especially the Storz system seemed to perform unpredictable non-linear processing before images are displayed. This affects the quantification, even if it is inflow-based. Although the healthy control group and impaired perfusion group were generally measured using different NIR systems, it is highly unlikely that this was solely responsible for the observed distinction in the clinical study. The in vitro experiments indicated that sudden exposure to high radiance mostly induces unexpected system behaviour, which is not the case during in vivo measurements. Second, and most importantly, revascularization in the impaired perfusion group caused restoring of inflow parameters into the healthy range. All things considered, the current results of the FLIGHT study cannot be directly applied for clinical decision-making, but enthusiasm regarding the potential of our developed system does not need to be tempered.

7.2 Future perspectives

As mentioned before, the presented work provides the *first steps* towards a clinically implementable tool for quantification of intestinal perfusion. Despite these steps being of great significance, plenty of room remains for improvement, especially before clinical implementation can be realised.

The clinical pilot study has provided a proof-of-concept, by illustrating the differences in inflow parameters between normal and compromised perfusion. However, for the purpose of intraoperative decision-making, threshold values need to be determined. It should be noted that, in the current situation, determining these values based on clinical outcome is not straightforward. Consider for example the situation that FA inflow parameters qualify a certain bowel segment as 'within healthy range', while the surgeon would perform a resection based on current best practice. Follow up information on perforation and necrosis is lost when bowel is resected. This complicates the demonstration of the technique's superiority over clinical judgement and the specification of threshold values. If the current observational FLIGHT study is expanded with more data that suggests superiority of quantified FA, a step towards clinical decision-making can be made in a trial setting. Ethical principles should then be considered carefully.

In our group, we envision a 'stoplight' system that, based on FA quantification, describes whether a certain area of tissue is either sufficiently perfused (green), insufficiently perfused (red) or dubiously perfused (orange). Naturally, the orange range, where clinical circumstances like extent of resection and short bowel syndrome need to be considered, should be as narrow as possible. Furthermore, these ranges are not consistent for all procedures, as wound healing (i.e. anastomosis), bowel salvage, and relieve of CMI symptoms all require different levels of perfusion. In this system, the stoplight colours would replace the current heatmap of the parametric mapping function.

Another crucial development is the implementation of the previously mentioned 'raw data'. In addition to the discussed effect on parameters, this could have another purpose. Chapter 6 discusses the fact that the current method of FA quantification still requires some amount of subjective interpretation, specifically in the event of very low perfusion levels. An intuitive downside to inflow-based quantification is the fact that they do not convert to zero when no ICG inflow is present. Instead, they are not defined. Moreover, in case of very low intensity levels, inflow-quantification is inaccurate. If information is available on the radiance measurements, it is easier to identify what causes the low intensity values (e.g. low perfusion or image processing).

The current software tool can be optimized for increased ease of use and effectiveness. Most importantly, computer vision techniques should be applied to correct for motion, both by the camera and the intestine itself. Not only does this reduce artefacts in measurements, it improves intraoperative use as well. Currently, integration of the parametric mapping into live footage is only possible when the camera is held still. Being able to correct for camera motion after FA will allow the quantification to be implemented seamlessly in the surgical workflow. Improved automatic segmentation algorithms are desired as well.

The work described in this thesis has taken the technology readiness of FA quantification from level 2-3 (basic research as described in previous literature) to level 4 (experimental pilot study).

The live analysis software has been demonstrated (level 5), albeit without validated algorithms. This external validation of the algorithms and imaging systems, with the help of more sophisticated perfusion phantoms, is an important next step. From here, clinical trials can be set up to pursue level 7.

A final important notion is that the developed technology could be extrapolated to perfusion measurements in other organs. Knowledge on perfusion dynamics is, for example, critical in the treatment of peripheral artery disease, but this technique could also be applied in other disciplines, such as plastic and cardiothoracic surgery.

To conclude, FA can be transformed into the clinically applicable tool for quantification of intestinal tissue perfusion that is so desperately needed. With its help, surgeons can get rid of intraoperative uncertainties, preventing complications for a great many patients.

Appendix A: Changepoint detection

Supplementary material of: ***Vaassen et al.*** *Fluorescence-based Quantification of Gastrointestinal Perfusion: A Step Towards an Automated Approach (2021)*

This document describes the processing steps in the detection of the start- and endpoint of intensity increase (T_0 and T_{max}) in a quantified fluorescence angiography (FA) signal. The intensity-time signal is acquired by measuring the mean pixel intensity in a specified region of interest for each timeframe of an FA video. The signal is subsequently filtered using a lowpass Butterworth filter (cut-off at 0.18 Hz).

First, candidate points are designated by a changepoint detection algorithm. The changepoints represent a point of significant change in linear trend of the signal. It is expected that the desired locations are among these changepoints. The search domain of the algorithm is set between a manually assigned starting frame s and the frame where the signal reaches its absolute maximum N. The algorithm utilizes the following steps:

Input: - Intensity signal $x(t)$ sampled as a vector in domain $D = \{s, N\}$: $(x_s, x_{s+1} \dots x_N)$.

- Number of changepoints to search for, i.e. the size of changepoint set K.

Iterate:

1. Set k as a changepoint, dividing x into sectors $(x_s \dots x_{k-1})$ and $(x_k \dots x_N)$.
2. Compute the deviation from optimal linearity of each sector, and sum to calculate residual error. This is performed by evaluating the cost function:

$$J(k) = \sum_{i=s}^{k-1}\left(x_i - \mu([x_s \dots x_{k-1}])\right)^2 - \frac{\left(\sum_{i=s}^{k-1}\left(x_i - \mu([x_s \dots x_{k-1}])\right) * \left(i - \mu([s \dots k-1])\right)\right)^2}{\sum_{i=s}^{k-1}\left(i - \mu([s \dots k-1])\right)^2}$$

$$+ \sum_{i=k}^{N}\left(x_i - \mu([x_k \dots x_N])\right)^2 - \frac{\left(\sum_{i=k}^{N}\left(x_i - \mu([x_k \dots x_N])\right) * \left(i - \mu([k \dots N])\right)\right)^2}{\sum_{k}^{N}\left(i - \mu([k \dots N])\right)^2} \qquad \text{(A. 1)}$$

   With $\mu(\vec{v})$ defined as the mean of a vector $(\vec{v})$ according to: $\mu(\vec{v}) = \frac{1}{n}\sum_{i=1}^{n} v_i$.

3. Minimize $J(k)$ by varying k. The process of minimizing this cost function is described in more detail in articles by Lavielle and Killick et al. [1,2]. In case of more than one changepoint, i.e. a set of changepoints K, cost function $J(K)$ will be a straightforward extension of $Eq.(A.1)$. Minimizing is then performed by varying all points in set K.

Output: Set of changepoints with respect to linear trend in K.

$Eq.(A.1)$ is suitable for the assessment of linearity in each candidate sector, since the error of each sector

$$E = \sum_{i=1}^{n}\left(x_i - \mu([x_1 \dots x_n])\right)^2 - \frac{\left(\sum_{i=1}^{n}\left(x_i - \mu([x_1 \dots x_n])\right) * \left(i - \mu([1 \dots n])\right)\right)^2}{\sum_{i=1}^{n}\left(i - \mu([1 \dots n])\right)^2}$$

$$= n * var(x) - \frac{n^2 * cov(x,t)^2}{n * var(t)} \quad \text{(A. 2)}$$

Using the Pearson correlation coefficient ($Eq.\,(A.3)$),

$$r_{x,t} = \frac{\sum_{i=1}^{n}\left(x_i - \mu([x_1 \dots x_n]) * \left(i - \mu([1 \dots n])\right)\right)}{\sqrt{\sum_{i=1}^{n}\left(x_i - \mu([x_1 \dots x_n])\right)^2} * \sqrt{\sum_{i=1}^{n}\left(i - \mu([1 \dots n])\right)^2}} = \frac{n * cov(x,t)}{\sqrt{n * var(x)} * \sqrt{n * var(t)}} \quad \text{(A. 3)}$$

$Eq.\,(2)$ can be rewritten as:

$$E = n * var(x) - n * var(x) * {r_{x,t}}^2 \quad \text{(A. 4)}$$

${r_{x,t}}^2$ approximates 1 when $x(t)$ can be closely described by a linear function, causing error E to approximate 0. Therefore, minimization of this function finds segments with optimal linearity. Accordingly, the borders of these segments represent changepoints in linear trend.

After a set of changepoints K has been established, final selection of T_0 and T_{max} is performed based on several conditions. These conditions are evaluated using the derivative of the signal segments between changepoints $x(K)$: $D(K) = \frac{dx}{dK}$. In order to find T_0, the algorithm selects the first changepoint k where the slope in three successive segments is above a certain threshold α. If none of the changepoints meet this condition, the first changepoint in set K is appointed as T_0. This condition relies on the fact that the actual intensity increase has an exponential trend in the very beginning. As a result, multiple changepoints are found in this area. The segments between

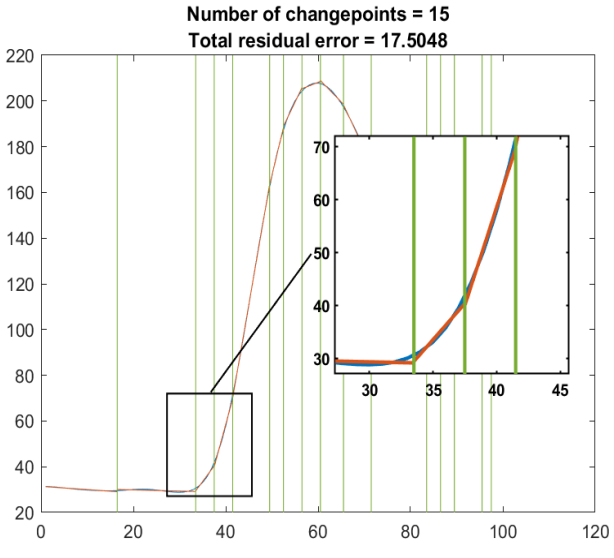

Fig. A.1. *Changepoint detection. The zoomed portion of the plot shows the exponential trend at T_0, resulting in the detection of multiple changepoints. The blue line represents the intensity signal and the orange lines represent the fitted trend lines.*

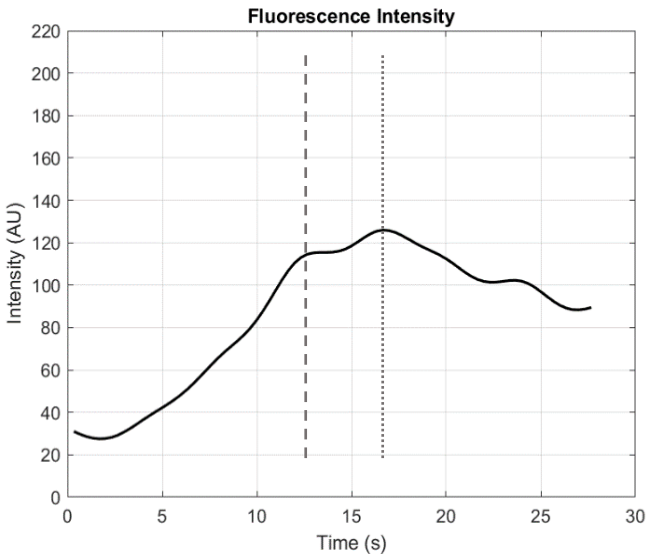

Fig. A.2. *Intensity-time curve presenting with two possible locations for T_{max}.*

them have an increasing linear slope (see Fig. A.1). This property is used by the algorithm to distinguish the actual T_0 from fluctuations in the baseline signal.

The selection of T_{max} is performed by finding the first point in K where the slope in the successive segment is below a threshold β, while $x(k)$ is not below 95% of the absolute maximum of the curve. This condition is utilized to cope with intensity plateaus after initial signal increase. Figure A.2 shows a frequently arising ambiguity with respect to T_{max}. Due to an intensity plateau with a slight successive peak, the true location of T_{max} becomes unclear. Rather than basing the selection on the overall maximal intensity value, the algorithm focusses on a significant 'end of increase'. It is believed that this results in more consistent and reliable measurements. Designation of a 'premature' end of increase is prevented by the 95% of maximal value threshold.

A total of five parameters can be varied to optimize the algorithm: the thresholds for the detection of T_0 $(\alpha_1, \alpha_{2,}\alpha_3)$ and the detection of T_{min} (β), as well as the number of changepoints to be found. Based on trial and error, these parameters were set as follows: $\alpha_1 = 2{,}1\ AU/s$, $\alpha_2 = 3{,}6\ AU/s$, $\alpha_3 = 3{,}6\ AU/s$, $\beta = 3{,}6\ AU/s$ and number of changepoints $|K| = 15$.

References

1. Lavielle M. Using penalized contrasts for the change-point problem. Signal Processing. 2005 Aug 1;85(8):1501–10.

2. Killick R, Fearnhead P, Eckley IA. Optimal detection of changepoints with a linear computational cost. J Am Stat Assoc [Internet]. 2012 Jan 7 [cited 2020 Jun 3];107(500):1590–8. Available from: http://arxiv.org/abs/1101.1438

Appendix B: Abstract for 35th Annual Meeting of the European Society for Vascular Surgery

Fluorescence Angiography for Peroperative Assessment of Bowel Viability in Patients with Mesenteric Ischemia

H.G.M. Vaassen BSc, B. Wermelink MSc, D.J. Lips MD. PhD, R.H. Geelkerken Prof. MD. PhD.

To be published in EJVES - Vascular Forum (Issue 53, 2021)

Introduction – Resection of inviable intestine after revascularization is often necessary in case of severe mesenteric ischemia. In current practice, blood supply and bowel viability are evaluated peroperatively by means of clinical observations such as mucosal colour, palpable pulsations and bleeding from the marginal artery. However, these methods lack accuracy and objectivity, irrespective of a surgeon's experience.[1] Low reproducibility and technical difficulties have prevented approaches using Doppler and laser speckle contrast imaging from reaching standard clinical implementation.[2–4] There is a need for objective and reliable peroperative detection of insufficient intestinal perfusion.
Fluorescence angiography (FA) through the use of Indocyanine-green has presented itself as a provider of valuable insights into local perfusion dynamics. Nevertheless, randomized control trials failed to show a reduction in anastomotic leakage after colorectal surgery when using FA.[5,6] This is most likely caused by the qualitative and subjective interpretation of the FA images. Quantified FA, based on an intensity-over-time signal, seems to be a promising and objective approach. However, as of yet there is no consensus on the acquisition and interpretation of quantified FA parameters. We propose the use of automated algorithms for objective and convenient FA interpretation.

Methods – We developed algorithms for the automatic extraction of inflow-based parameters, specifically the time to reach 50% of maximal intensity ($T_{1/2}$) and the maximal normalized slope (slp_n). (see Fig. B.1). These parameters are more reliable than direct intensity measurements and provide an improved reflection of clinical endpoints.[7] A changepoint detection algorithm was developed for extracting the start- and endpoint of intensity increase, allowing for calculation of $T_{1/2}$. Slope of the signal was determined using a least squares approximation, in order to deal with signal noise.
FA was performed on the small intestine of 38 subjects with normally expected intestinal perfusion. The performance of the changepoint detection algorithm was evaluated against manual extraction.

Results – Automated quantitative FA was feasible in all subjects. The changepoint detection algorithm produced very similar results to manual extraction (Intraclass Correlation = 0.95). $T_{1/2}$ had a median value of 5.1 (interquartile range = 2.4) seconds. Median value of slp_n was 18.5 (interquartile range = 8.4) %/second. To illustrate the added value of an automated approach, cartograms based on slp_n were developed (see Figure B.2).

Conclusion – The proposed method of using quantified FA for the peroperative assessment of intestinal perfusion is objective, convenient and seems very promising. An automated approach

allows for the generation of immersive cartograms and thus direct access to objective information regarding bowel viability after vascular reconstruction.
At this point in time, measurements are being performed on patients suffering from mesenteric ischemia. The quantified FA parameters will be compared with a newly developed bowel viability scoring system and with clinical outcome. This way, the correct interpretation of FA parameters and their predictive value will be elucidated.

NB: The method for extracting $T_{1/2}$ has recently been published online:
https://doi.org/10.1089/lap.2021.0102

This abstract contains new information from a study following this publication.

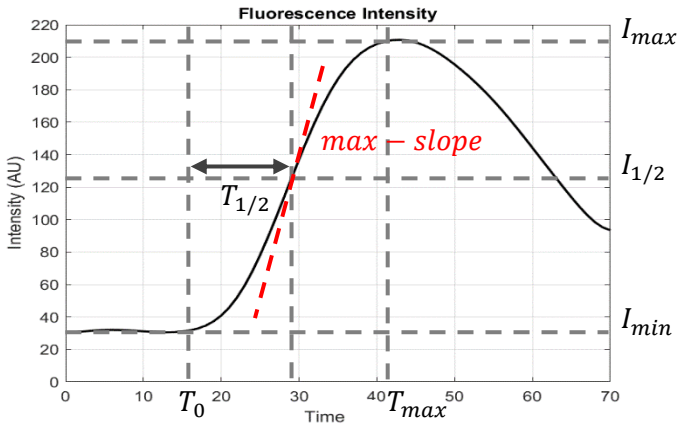

Figure B.1. *Filtered intensity-time curve of FA. $T_{1/2}$ is defined as the time between first intensity increase and the point of reaching 50% of maximal intensity. Maximum slope is normalized to slp_n by dividing by $(I_{max} - I_{min})$.*

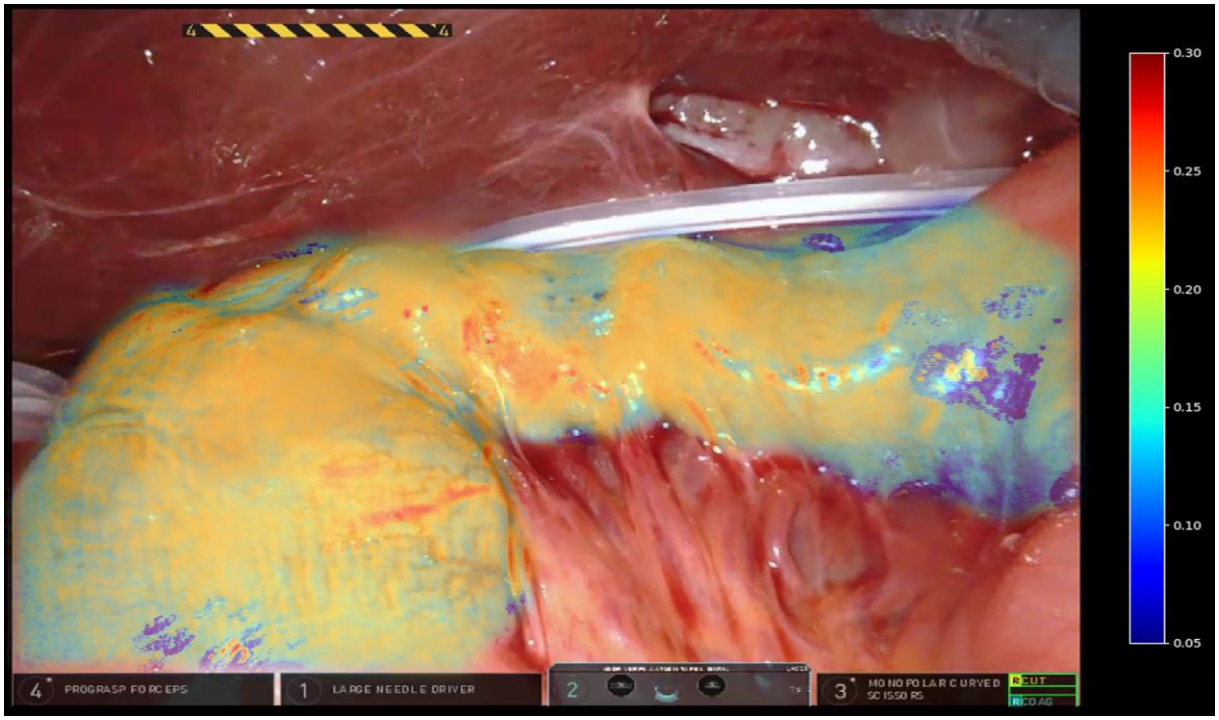

Figure B.2. *Cartogram merged into white-light laparoscopic image, displaying the maximal normalized slope value for each pixel.*

References

1. Karliczek A, Harlaar NJ, Zeebregts CJ, Wiggers T, Baas PC, van Dam GM. Surgeons lack predictive accuracy for anastomotic leakage in gastrointestinal surgery. Int J Colorectal Dis. 2009;24(5):569-576.

2. Kawada K, Hasegawa S, Wada T, et al. Evaluation of intestinal perfusion by ICG fluorescence imaging in laparoscopic colorectal surgery with DST anastomosis. Surg Endosc. 2017;31(3):1061-1069.

3. Wada T, Kawada K, Takahashi R, et al. ICG fluorescence imaging for quantitative evaluation of colonic perfusion in laparoscopic colorectal surgery. Surg Endosc. 2017;31(10):4184-4193.

4. Rønn JH, Nerup N, Strandby RB, et al. Laser speckle contrast imaging and quantitative fluorescence angiography for perfusion assessment. Langenbeck's Arch Surg. 2019;404(4):505-515.

5. De Nardi P, Elmore U, Maggi G, et al. Intraoperative angiography with indocyanine green to assess anastomosis perfusion in patients undergoing laparoscopic colorectal resection: results of a multicenter randomized controlled trial. Surg Endosc. 2020;34(1):53-60.

6. Alekseev M, Rybakov E, Shelygin Y, Chernyshov S, Zarodnyuk I. A study investigating the perfusion of colorectal anastomoses using fluorescence angiography: results of the FLAG randomized trial. Color Dis. 2020;22(9):1147-1153.

7. Lütken CD, Achiam MP, Svendsen MB, Boni L, Nerup N. Optimizing quantitative fluorescence angiography for visceral perfusion assessment. Surg Endosc. 2020;34(12):5223-5233.

Appendix C: Cover letter for video case-report

Fluorescence Angiography to Assess Intestinal Viability during Emergency Laparoscopy for Small Bowel Obstruction – A Video Correspondence

H.G.M. Vaassen BSc, J. Sprakel MD, D.J. Lips MD. PhD

Ready for submission

Dear Editor,

Intestinal perfusion and viability are largely assessed intraoperatively by means of the clinical eye. However, this method lacks objectivity and accuracy, irrespective of a surgeon's experience.[1] Fluorescence angiography (FA) provides direct insights into microvascular perfusion, and might be of aid in this issue.

We present the case of a 63-year old male patient who was admitted at the Emergency Department with severe abdominal pain and vomiting. He was diagnosed with small bowel obstruction on CT and underwent exploratory laparoscopy.

First inspection inside the abdomen revealed a herniation of the small intestine into a defect in the falciform ligament. The affected bowel showed significant signs of ischemia, based on which an experienced GE surgeon planned a bowel resection. However, FA displayed impaired, but evident, arterial inflow. After release of the strangulation, FA was performed once more. At this point, the affected bowel showed a noticeable arterial inflow as well as venous outflow, in very close resemblance to neighbouring healthy intestine. Based on these findings, the ischemia was deemed not irreversible and the decision was made to postpone the resection and end the procedure. The patient could be discharged six days after surgery without complications.

In our opinion, the future of FA lies in objective quantification. Retrospective analysis of FA images showed that state-of-art quantification of fluorescence inflow dynamics reflected the clinical recovery of ischemic bowel. Future research should focus on establishing threshold values for the prediction of bowel viability, transforming FA into an objective decision-making system.

References

1. Karliczek A, Harlaar NJ, Zeebregts CJ, Wiggers T, Baas PC, van Dam GM. Surgeons lack predictive accuracy for anastomotic leakage in gastrointestinal surgery. Int J Colorectal Dis. 2009;24(5):569-576.

Appendix D: Clinical score of intestinal ischemia

Clinical judgement	Visual	Score	Palpation	Score	Doppler	Score
Reversible, non-transmural ischemia most likely	- Pale pink colour. - Visible serosal vasculature. - Observable peristalsis	*V-I*	- Firm bowel wall, slight oedema allowed. - Palpable pulsations in arcade.	*P-I*	- Clear signals up to arcade.	*D-I*
Reversibility of bowel wall ischemia uncertain	- Colour transitioning from pink to grey. - Dubious serosal vasculature.	*V-II*	- Oedematous, locally thinned but resilient bowel wall. - No palpable pulsations in arcade.	*P-II*	- Dubious/weak signals.	*D-II*
Irreversible, transmural ischemia/necrosis most likely	- Black/grey/green colour. - No serosal vasculature. - No peristalsis.	*V-III*	- Thin, fragile bowel wall. - No pulsation.	*P-III*	- No arterial signals.	*D-III*